

$\gamma^*N \rightarrow N^*(1520)$ form factors in the spacelike region

G. Ramalho¹ and M. T. Peña²

¹*International Institute of Physics, Federal University of Rio Grande do Norte, Avenida Odilon Gomes de Lima 1722, Capim Macio, Natal-RN 59078-400, Brazil* and

²*Centro de Física Teórica de Partículas (CFTP), Instituto Superior Técnico (IST), Universidade de Lisboa, Avenida Rovisco Pais, 1049-001 Lisboa, Portugal*

(Dated: August 23, 2018)

The covariant spectator quark model is applied to the $\gamma^*N \rightarrow N^*(1520)$ reaction in the spacelike region. The spin quark core contributions to the electromagnetic form factors and helicity transition amplitudes are estimated from the covariant structure of the $N^*(1520)$ wave function calibrated by the experimental data for large squared momentum transfer Q^2 . The difference between the model results and the experimental data is then used to parametrize the low Q^2 behavior, where meson cloud effects are assumed to dominate. This parametrization can be very useful for future studies of the reaction, as well as for the extension of the transition form factors to the timelike region.

I. INTRODUCTION

The electromagnetic structure of the hadrons and its connection to Quantum ChromoDynamics is one of the most interesting topics of investigation in hadronic physics. Recently, accurate data involving nucleon resonances (baryons) was extracted from experiments at low and high Q^2 ($Q^2 = -q^2$, where q is the momentum transfer), in such facilities as Jefferson Lab (Jlab) and MAMI (Mainz) [1, 2], demanding theoretical interpretations. These experiments access the electromagnetic structure of several baryons through the scattering of electrons off nucleons (N), inducing nucleon electro-excitation reactions ($eN \rightarrow e'N^*$). These electroproduction reactions proceed through the intermediate step $\gamma^*N \rightarrow N^*$, where γ^* is a virtual photon, with a cross section that can be written in terms of electromagnetic form factors.

The pattern of the excitation of the nucleon resonances N^* is observed in the total cross section as a function of the γ^*N invariant mass W , and the first excitation is clearly characterized by the bump around $W \simeq 1.2$ GeV, identified as the state $\Delta(1232)$, which defines the first resonance region. For a review about the $\Delta(1232)$ see Refs. [1, 3–5]. The second bump is a combination of several resonances, dominated by the $N^*(1520)$ and $N^*(1535)$ states. This last one was already studied in some detail (see Ref. [6] and references therein). Here we will study the state $N^*(1520)$, and the $\gamma^*N \rightarrow N^*(1520)$ transition.

The $N^*(1520)$ has spin $3/2$ and negative parity ($J^P = \frac{3}{2}^-$). In the context of πN scattering it contributes to the $D_{13}(1520)$ channel, with isospin $1/2$ and spin $3/2$ and πN relative orbital momentum $l = 2$. The $\gamma^*N \rightarrow N^*(1520)$ reaction is therefore characterized by three independent helicity amplitudes, usually defined in the final state rest frame: the two transverse amplitudes $A_{1/2}$, $A_{3/2}$, and the

longitudinal amplitude $S_{1/2}$. Only recently was the longitudinal amplitude measured for the first time [7, 8]. In the timelike region ($Q^2 < 0$) the $N^*(1520)$ state also has a relevant contribution to the dilepton decay reactions ($\gamma^*N \rightarrow e^+e^-N$) [9–12].

The $\gamma^*N \rightarrow N^*(1520)$ was studied previously within the framework of nonrelativistic and relativistic quark models [13–22], the single quark transition model (SQTm) [23–25] and a collective model for baryons [26]. The electromagnetic structure of the $N^*(1520)$ was also estimated by the EBAC (Jlab) analysis, within a coupled-channel dynamical model for the meson-baryon systems [27]. The study of the empirical charge density distribution for the $N^*(1520)$ can be found in Refs. [28, 29]. From the experimental side, there are the MAID (Mainz) analysis [28–30], the old data from DESY [31] and NINA [32], and the recent data from CLAS (at Jlab) [7, 8]. For a review of results see Refs. [1, 7, 8].

In this work we will study the $\gamma^*N \rightarrow N^*(1520)$ transition using the covariant spectator quark model [33–37], which is based on the so-called covariant spectator theory [38]. This model was already applied to the electromagnetic structure of the nucleon [33, 36, 37, 39] and the $\Delta(1232)$ [4, 5, 39–41], $N^*(1440)$ [42], $N^*(1535)$ [6, 43], $\Delta(1600)$ [44], the baryon octet and decuplet [34, 45–47] and other transitions [48, 49]. The model was also applied to the timelike regime for the $\Delta(1232)$ case, in particular to the calculation of the Δ dielectron Dalitz decay [50].

In the calculations of the transition electromagnetic form factors of the $\gamma^*N \rightarrow N^*(1520)$ reaction we use the relativistic impulse approximation, as done in previous works [4, 5, 34, 39–41, 46, 47] on different reactions. In this approximation each quark interacts with the photon at a time, implying that the electromagnetic probe does not couple simultaneously with two or three quarks. In our model the single quark electromagnetic

form factor parametrizes the quark dressing from quark-antiquark pairs and gluons, reproducing the quark charge and generating an anomalous magnetic moment. This means that meson effects are effectively taken at the level of (dressing) one quark only, but processes where the meson is exchanged between different quarks, and therefore is emitted and absorbed collectively by the three quarks, by the baryon as a whole, are not included [46, 49]. Throughout this paper these are the effects we refer to when we use the term "meson cloud". We discuss next the motivation to add these effects to the contributions from our covariant spectator quark model.

For the $\Delta(1232)$ excitation [4, 5, 39–41] the comparison of our results to the data has shown that these meson cloud effects are important in the small Q^2 region. This conclusion is shared with other constituent quark models [1, 3]. Namely, our results for the Δ electro-excitation are in line with the information on the pion cloud extracted within a dynamical coupled-channel analysis of an extensive collection of data [27, 51]. Besides, the same conclusion was obtained by a less phenomenological calculation, the dynamical quark calculation based on the Dyson-Schwinger framework [52] which used an underlying dynamics to generate the diquark propagation, and included the photon coupling to the diquark. Even with these features, that calculation could not describe the experimental data for the $\gamma^*N \rightarrow \Delta(1232)$ magnetic form factor in the small Q^2 region, pointing to the importance of meson cloud effects at the baryon level, as our calculation did.

Turning to the $\gamma^*N \rightarrow N^*(1520)$ reaction, in this work we start by writing the $N^*(1520)$ wave function in spin-flavor and momentum space by imposing the correct symmetries as described in Refs. [1, 53]. This wave function is the superposition of two configurations: one configuration where the quark core is a $S = 1/2$ spin state, and another where the quark core is a $S = 3/2$ spin state. The mixture coefficient for the $S = 3/2$ configuration has been estimated to be $\sin \theta_D \approx 0.1$, suggesting a dominance of the $S = 1/2$ configuration [1, 14]. In our work we confirmed the importance of the $S = 1/2$ configuration.

Our results for the helicity amplitudes at low Q^2 are too small when compared to the data. This seems to indicate that the meson cloud effects not included in our quark core model play a relevant role for the $N^*(1520)$, as they do for the $\Delta(1232)$. The $N^*(1520)$ decay to πN (60%) and $\pi\pi N$ (40%) [1], gives us already an indication that diagrams where the photon couples to a meson in flight in an intermediate baryon-meson state may very well be important for the $\gamma^*N \rightarrow N^*(1520)$ reaction, and point to the importance of the meson cloud contributions at the baryon level.

By comparing our results to the data, we extract a simple parametrization of their difference, that we interpret then as meson cloud contributions. This parametrization will be very useful in the extension of our calculation to the timelike region, which will enable us to interpret

dilepton production data from NN collisions [11, 12].

This article is organized as follows: In Sec. II we present the formalism required to parametrize the electromagnetic structure of the $\gamma^*N \rightarrow N^*(1520)$ reaction. The covariant spectator quark model for the baryon quark cores and the baryon effective wave functions necessary to calculate the transition are presented in Secs. III and IV. In Sec. V we derive the results for the form factors and helicity amplitudes, and discuss how to parametrize the meson cloud contributions. Details are presented in Appendices A to E. The numerical results for form factors and helicity amplitudes are presented in Sec. VI. Final conclusions are presented in Sec. VII.

II. FORMALISM

We start by introducing the formalism required for the study of the $\gamma^*N \rightarrow N^*(1520)$ transition. In what follows we will often represent $N^*(1520)$ as R (from resonance), and will use M for the nucleon mass and M_R for the resonance R mass. We will present the definitions of the helicity amplitudes $A_{3/2}$, $A_{1/2}$ and $S_{1/2}$ (which are experimentally determined) together with their relation to the electromagnetic transition form factors, G_M , G_E and G_C .

A. Helicity amplitudes

The electromagnetic transition from a $J^P = \frac{1}{2}^+$ state to a $J^P = \frac{3}{2}^-$ state is described by three amplitudes. They are functions of Q^2 , and in the R rest frame they are defined as [1]:

$$A_{3/2} = \sqrt{\frac{2\pi\alpha}{K}} \langle R, S'_z = +\frac{3}{2} | \epsilon_+ \cdot J | N, S_z = +\frac{1}{2} \rangle \quad (2.1)$$

$$A_{1/2} = \sqrt{\frac{2\pi\alpha}{K}} \langle R, S'_z = +\frac{1}{2} | \epsilon_+ \cdot J | N, S_z = -\frac{1}{2} \rangle \quad (2.2)$$

$$S_{1/2} = \sqrt{\frac{2\pi\alpha}{K}} \langle R, S'_z = +\frac{1}{2} | \epsilon_0 \cdot J | N, S_z = +\frac{1}{2} \rangle \frac{|\mathbf{q}|}{Q}, \quad (2.3)$$

where S'_z (S_z) is the final (initial) spin projection, \mathbf{q} is the photon three-momentum in the rest frame of R , $Q = \sqrt{Q^2}$, ϵ_λ^μ ($\lambda = 0, \pm 1$) are the photon polarization vectors and J^μ is the electromagnetic transition current in proton charge e units. In the previous equations $\alpha \simeq 1/137$ is the fine-structure constant and $K = \frac{M_R^2 - M^2}{2M_R}$ is the magnitude of the photon momentum (and nucleon) when $Q^2 = 0$. In the rest frame of R the magnitude of the

nucleon three-momentum is $|\mathbf{q}|$, and reads

$$|\mathbf{q}| = \frac{\sqrt{Q_+^2 Q_-^2}}{2M_R}, \quad (2.4)$$

where $Q_\pm^2 = (M_R \pm M)^2 + Q^2$.

The transition current J^μ for the reaction $\gamma^* N \rightarrow N^*(1520)$ between an initial nucleon state with momentum P_- , and a final R state with momentum P_+ can be represented in terms of the matrix elements J_{NR}^μ defined by the asymptotic states, and given by

$$\begin{aligned} J_{NR}^\mu &\equiv \langle R | J^\mu | N \rangle \\ &= \bar{u}_\beta(P_+) \Gamma^{\beta\mu} u(P_-), \end{aligned} \quad (2.5)$$

where u_β , u are respectively the Rarita-Schwinger and Dirac spinors. The operator $\Gamma^{\beta\mu}$ has the general Lorentz structure

$$\Gamma^{\beta\mu} = G_1 q^\beta \gamma^\mu + G_2 q^\beta P^\mu + G_3 q^\beta q^\mu - G_4 g^{\beta\mu}, \quad (2.6)$$

where $q = P_+ - P_-$ is the transferred momentum and $P = \frac{1}{2}(P_+ + P_-)$. In the previous equation G_i ($i = 1, \dots, 4$) are form factor functions that depend on Q^2 . Because of current conservation only three of the four G_i form factors are independent, and one is free to choose which three are to be taken as independent. For instance, from the knowledge of G_i ($i = 1, \dots, 3$), G_4 is determined by the current conservation condition $q_\mu J^\mu = 0$ as

$$G_4 = (M_R - M)G_1 + \frac{1}{2}(M_R^2 - M^2)G_2 - Q^2 G_3. \quad (2.7)$$

Note that there are alternative representations of the operator $\Gamma^{\beta\mu}$. They are all however equivalent to the ones given by Eq. (2.6) [1, 54]. Using (2.5)-(2.6) we can write the amplitudes (2.1)-(2.3) as [1, 55]

$$A_{1/2} = 2\mathcal{A} \left\{ G_4 - [(M_R - M)^2 + Q^2] \frac{G_1}{M_R} \right\}, \quad (2.8)$$

$$A_{3/2} = 2\sqrt{3}\mathcal{A}G_4, \quad (2.9)$$

$$S_{1/2} = -\frac{1}{\sqrt{2}} \frac{|\mathbf{q}|}{M_R} \mathcal{A} g_C, \quad (2.10)$$

where $\mathcal{A} = \frac{\epsilon}{4} \sqrt{\frac{(M_R + M)^2 + Q^2}{6MM_R K}}$, and

$$\begin{aligned} g_C &= 4M_R G_1 + (3M_R^2 + M^2 + Q^2)G_2 \\ &\quad + 2(M_R^2 - M^2 - Q^2)G_3. \end{aligned} \quad (2.11)$$

The obtained formulas for the helicity amplitudes suggest that for the $\gamma^* N \rightarrow N^*(1520)$ reaction it is convenient to choose as independent functions the three form factors G_1 , G_4 and g_C . Equations (2.7) and (2.11) can be used to express G_2 and G_3 in terms of those three quantities. In addition, one concludes that if $G_4 = 0$ then $A_{3/2}$ vanishes identically. Experimentally one has that $A_{3/2} \neq 0$, particularly at low Q^2 , and therefore the data demand $G_4 \neq 0$.

B. Electromagnetic form factors

Instead of the helicity amplitudes defined in the rest frame of R , or instead of the form factors G_i , one may also use the three so-called multipole electromagnetic form factors. Those are, in the present case the magnetic dipole G_M , the electric quadrupole G_E and the Coulomb quadrupole G_C . They can be written as combinations of the helicity amplitudes or the form factors G_i defined above, as [1]

$$\begin{aligned} G_M &= -F \left(\frac{1}{\sqrt{3}} A_{3/2} - A_{1/2} \right) \\ &= -\mathcal{R} [(M_R - M)^2 + Q^2] \frac{G_1}{M_R}, \end{aligned} \quad (2.12)$$

$$\begin{aligned} G_E &= -F \left(\sqrt{3} A_{3/2} + A_{1/2} \right) \\ &= -\mathcal{R} \left\{ 2G_4 - [(M_R - M)^2 + Q^2] \frac{G_1}{M_R} \right\}, \end{aligned} \quad (2.13)$$

$$G_C = 2\sqrt{2} \frac{M_R}{|\mathbf{q}|} F S_{1/2} = -\mathcal{R} g_C, \quad (2.14)$$

where $F = \frac{1}{e} \frac{M}{|\mathbf{q}|} \sqrt{\frac{MK}{M_R} \frac{(M_R - M)^2 + Q^2}{(M_R - M)^2}}$ and $\mathcal{R} = 2\mathcal{A}F$. We can also write $\mathcal{R} = \frac{1}{\sqrt{6}} \frac{M}{M_R - M}$.

Combining (2.12) and (2.13), one obtains

$$G_M + G_E = -2\mathcal{R}G_4. \quad (2.15)$$

When the form factors G_M and G_E are known the helicity amplitudes become

$$A_{1/2} = +\frac{1}{4F} (3G_M - G_E) \quad (2.16)$$

$$A_{3/2} = -\frac{\sqrt{3}}{4F} (G_M + G_E). \quad (2.17)$$

Defining

$$G'_4 = -2\mathcal{R}G_4, \quad (2.18)$$

one has

$$A_{1/2} = \frac{1}{F} G_M + \frac{1}{4F} G'_4 \quad (2.19)$$

$$A_{3/2} = \frac{\sqrt{3}}{4F} G'_4. \quad (2.20)$$

From Eqs. (2.12), (2.13), and (2.15), we conclude that G_E and G_M are determined by G_1 and G_4 only; G_1 fixes G_M ; G_4 fixes the sum $G_M + G_E$. We conclude, as it happened for the helicity amplitudes, that it is also convenient for the description in terms of G_E , G_M and G_C , to choose as independent functions G_1 (or G_M , since they are proportional), G_4 and g_C . Additionally, a result to be retained from these formulas is that when $G_4 = G'_4 = 0$, one has $G_M = -G_E$ (which is equivalent to $A_{3/2} \equiv 0$) for any value of Q^2 . Note that the relation $G_M = -G_E$ is not confirmed experimentally (because $A_{3/2} \neq 0$).

III. ELECTROMAGNETIC CURRENT

In the calculation of the baryon transition electromagnetic form factors we use the relativistic impulse approximation. In this approximation only one quark interacts with the photon while the other two quarks are spectators, but the electromagnetic interaction is distorted by the initial and final state baryon vertices, defining a Feynman diagram with one loop integration. First, one notes that within impulse approximation the relative momentum of the two quarks not interacting with the photon can be integrated over, since it does not depend on the electromagnetic interaction. (This is why for the calculation of the impulse diagram one may start with an effective wave function with a quark-diquark structure.) Second, when performing that integration we apply the covariant spectator theory to reduce in a covariant way the four dimensional integration to a three dimensional one.

This reduction amounts to select for the energy integration only the positive energy poles of the two quarks in the diquark. The consequence is that after the internal diquark three-momentum is integrated out, one ends up with on-mass-shell diquark with an averaged invariant mass m_D [33, 34, 36]. The selected quark poles dominate in the energy integration. The residues of the other poles (from the two propagators of the interacting quark, before and after its interaction with the photon) give the off-mass-shell diquark contribution. Their contribution is indeed small due to the large value of the baryon mass that decisively determines the relative location of all the poles in the complex plane [56].

If one represents the initial and final baryon wave functions by $\Psi_N(P_-, k)$ and $\Psi_R(P_+, k)$, where P_- is the N momentum, P_+ is the R momentum, and k the diquark momentum, the electromagnetic current in relativistic impulse approximation is given by [33, 34, 36]

$$J_{NR}^\mu = 3 \sum_{\Gamma} \int_k \bar{\Psi}_R(P_+, k) j_q^\mu \Psi_N(P_-, k), \quad (3.1)$$

where j_q^μ is the quark current associated with one quark only (the factor 3 takes into account the contributions of the other quarks demanded by symmetry), and the sum is over the diquark spin states Γ , including a diquark scalar component and a diquark vector component with polarization $\Lambda = 0, \pm$. The integral symbol $\int_k \equiv \int \frac{d^3\mathbf{k}}{2E_D(2\pi)^3}$ stands for the covariant integration in the diquark three-momentum \mathbf{k} , with $E_D = \sqrt{m_D^2 + \mathbf{k}^2}$. The single constituent quark current j_q^μ is decomposed into two terms

$$j_q^\mu = j_1 \hat{\gamma}^\mu + j_2 \frac{i\sigma^{\mu\nu} q_\nu}{2M}, \quad (3.2)$$

where M is again the nucleon mass, j_1 and j_2 are the Dirac and Pauli quark operators and

$$\hat{\gamma}^\mu = \gamma^\mu - \frac{\not{q} q^\mu}{q^2}. \quad (3.3)$$

The inclusion of the last term is equivalent to using the Landau prescription for the electromagnetic current and ensures the conservation of J_{NR}^μ [57–59]. Equation (3.2) is a simple prescription that builds in current conservation in calculations within impulse approximation for inelastic processes with a pure phenomenological description of the final and initial states. It overcomes the difficulty that these states and the consistent interaction current are not calculated from an underlying dynamics [57]. Reference [58] also shows that the inclusion of the term $-\not{q} q^\mu / q^2$ does not affect the results for the observables because it is orthogonal to the lepton current.

The quark form factors j_i ($i = 1, 2$) have an isoscalar and an isovector component, given respectively by the functions f_{i+} and f_{i-} (of Q^2),

$$j_i = \frac{1}{6} f_{i+} + \frac{1}{2} f_{i-} \tau_3. \quad (3.4)$$

The explicit forms of the Dirac and Pauli quark form factors, $f_{1\pm}$ and $f_{2\pm}$ respectively, are chosen to be consistent with the vector meson dominance (VMD) mechanism, being parametrized as [4, 33, 34]

$$\begin{aligned} f_{1\pm}(Q^2) &= \lambda_q + (1 - \lambda_q) \frac{m_v^2}{m_v^2 + Q^2} + c_\pm \frac{M_h^2 Q^2}{(M_h^2 + Q^2)^2} \\ f_{2\pm}(Q^2) &= \kappa_\pm \left\{ d_\pm \frac{m_v^2}{m_v^2 + Q^2} + (1 - d_\pm) \frac{M_h^2}{M_h^2 + Q^2} \right\}, \end{aligned} \quad (3.5)$$

where m_v is a light vector meson mass, M_h is a mass of an effective heavy vector meson, κ_\pm are quark anomalous magnetic moments, c_\pm, d_\pm are mixture coefficients and λ_q is a parameter related with the quark density number in deep inelastic scattering.

The quark form factors are normalized according to $f_{1\pm}(0) = 1$ and $f_{2\pm}(0) = \kappa_\pm$, with the quark isoscalar (κ_+) and isovector (κ_-) magnetic moments given in terms of the u and d quark anomalous moments as $\kappa_+ = 2\kappa_u - \kappa_d$ and $\kappa_- = \frac{1}{3}(2\kappa_u + \kappa_d)$. In the applications we took $m_v = m_\rho$ ($\simeq m_\omega$) to include the physics associated with the ρ -pole and $M_h = 2M$ (twice the nucleon mass) to take into account effects of meson resonances with a larger mass. We consider here the parametrization that is consistent with the model for the nucleon labeled model II in Ref. [33]. The current parameters are $c_+ = 4.16$, $c_- = 1.16$, $d_+ = d_- = -0.686$, $\lambda_q = 1.21$, $\kappa_+ = 1.639$ and $\kappa_- = 1.833$.

IV. BARYON WAVE FUNCTIONS

In the covariant spectator quark-diquark model the diquark states are described in terms of diquark polarization vector states $\varepsilon_{\Lambda P}^\alpha$, where $\Lambda = 0, \pm$ are the polarization indices, which are expressed in the basis of fixed-axis states [4, 33, 60]. For a resonance R with momentum

$P = (E_R, 0, 0, P_z)$ the diquark polarization states read

$$\begin{aligned}\varepsilon_{\pm P}^\alpha &= \mp \frac{1}{\sqrt{2}}(0, 1, \pm i, 0) \\ \varepsilon_{0P}^\alpha &= \frac{1}{M_R}(P_z, 0, 0, E_R),\end{aligned}\quad (4.1)$$

where $E_R = \sqrt{M_R^2 + P_z^2}$ is the resonance energy. The same form applies to the nucleon if one replaces $M_R \rightarrow M$. Note that the polarization vectors depend on both the baryon mass and the baryon momentum, and satisfy the condition $\varepsilon_{\Lambda P} \cdot P = 0$.

The core spin 3/2 state are represented by the Rarita-Schwinger vector state u_α , and the core spin 1/2 are represented by the combination of a spin-1 (diquark) and a Dirac spin 1/2 states that reads

$$U_R^\alpha(P, s) = \frac{1}{\sqrt{3}}\gamma_5 \left(\gamma^\alpha - \frac{P^\alpha}{M_R} \right) u_R(P, s), \quad (4.2)$$

where u_R is the Dirac spinor for the particle R [4, 33]. Within this formalism, the wave functions for several baryon systems can be written in terms of the states U_R^α , u_R and u_β [4, 33–36]. These building blocks make possible the construction of baryon wave functions that are explicitly covariant and have the correct nonrelativistic limit [4, 33].

Next we will review the formulas for the nucleon wave function, and we will obtain the $N^*(1520)$ wave function.

A. Nucleon wave function

In the simplest covariant spectator model for the nucleon wave function, one takes an S -state for the quark-diquark configuration. In that configuration, the nucleon wave function has a form imposed by demanding that the full wave function is symmetric under the exchange of any two quarks in momentum-spin and flavor space. One has then [33, 36, 60]

$$\Psi_N(P, k) = \frac{1}{\sqrt{2}} [\phi_I^0 u(P) - \phi_I^1 (\varepsilon_{\Lambda P}^*)_\alpha U^\alpha(P)] \psi_N(P, k), \quad (4.3)$$

The first and the second terms are, respectively, the contributions from the scalar (spin-0, isospin-0) and from the axial vector (spin-1, isospin-1) diquark states. In addition, $\phi_I^{0,1}$ are the nucleon isospin states [33], u is the Dirac spinor, and U^α is the state defined by Eq. (4.2) in the special case of the nucleon ($M_R \rightarrow M$). It corresponds to the coupling of the spectator quark with a spin-1 vector diquark state to a three-constituent quark core state of spin 1/2. The vector $\varepsilon_{\Lambda P}$, where $\Lambda = 0, \pm 1$, is the diquark polarization state, introduced before. Finally, ψ_N is a radial wave function which encodes the information on the quark-diquark relative momentum distribution. It was determined phenomenologically [33].

The nucleon spin and isospin projections and the diquark polarization index Λ were not included explicitly in Eq. (4.3), to keep a short-hand notation. The spin projections were also omitted in the spin states u and U^α .

B. $N^*(1520)$ wave function

Since the $N^*(1520)$ has intrinsic negative parity and total spin $J = 3/2$, its wave function is a mixture of two contributions, Ψ_{R1} and Ψ_{R3} , with total orbital angular momentum $L = 1$, coupled respectively to states with core spin 1/2 and states with core spin 3/2. One writes then for the $N^*(1520)$ wave function [1, 14, 19]

$$\Psi_R(P, k) = \cos \theta_D \Psi_{R1}(P, k) - \sin \theta_D \Psi_{R3}(P, k), \quad (4.4)$$

where the two components are normalized. The admixture parameter, given by the angle θ_D depends on the model for the quark-quark interaction, and can be determined from the radiative decay of the resonances $N^*(1520)$ and $N^*(1700)$ (both $\frac{3}{2}^-$ states) [24, 61, 62]. The most common estimate is $\sin \theta_D \simeq 0.11$ [24, 53].

To write the components Ψ_{R1} and Ψ_{R3} in the covariant spectator quark model we will start with the nonrelativistic form, and discuss afterward how the nonrelativistic structure (in the rest frame) is obtained, and written in a covariant form valid in an arbitrary frame.

1. Nonrelativistic wave functions

In what follows, and as usual in the literature, we denote each wave function component by its symmetry labels (ρ, λ) . These labels coincide with the symmetry labels of the two Jacobi momentum states (k_ρ, k_λ) , respectively antisymmetric and symmetric in the change of quarks (12), and defined as

$$\begin{aligned}k_\rho &= \frac{1}{\sqrt{2}}(k_1 - k_2), \\ k_\lambda &= \frac{1}{\sqrt{6}}(k_1 + k_2 - 2k_3) \\ &= \sqrt{\frac{2}{3}}(k_1 + k_2) - \frac{1}{\sqrt{6}}P,\end{aligned}\quad (4.5)$$

where k_i is the individual momenta ($i = 1, 2, 3$), and $P = k_1 + k_2 + k_3$, is the center of mass momentum. In the nonrelativistic framework all the momenta introduced are three-vectors, although we will use later the same notation to represent their four-vector counterparts.

In the center of mass frame, $\mathbf{P} = \mathbf{0}$, k_λ becomes proportional to $k_1 + k_2$, and one can describe the system by the variables r and k , as

$$\begin{aligned}k_\rho \rightarrow r &= \frac{1}{2}(k_1 - k_2) \\ k_\lambda \rightarrow k &= k_1 + k_2.\end{aligned}\quad (4.6)$$

In the construction of the wave function components Ψ_{R1} and Ψ_{R3} , instead of using the basis of states corresponding to the Jacobi-momentum states of the three-quark system, we follow the usual practice in calculations of the baryon spectra, and take a representation of those baryon states in a basis that combines the Jacobi-momentum states into four (orthogonal) states with mixed-symmetry in the Jacobi momentum-spin and isospin variables [53]. These four combinations are built to be either symmetric or antisymmetric in the interchange of quarks 1 and 2. In such a basis the $N^*(1520)$ corresponds to the following isospin-spin-momentum combination [53],

$$\Psi_{Ri} = N_{Ri} [\phi_I^0 X_\rho + \phi_I^1 X_\lambda] \tilde{\psi}_{Ri}, \quad (4.7)$$

where Ri stands for $R1$ and $R3$ and N_{Ri} is a normalization factor, $\phi_I^{0,1}$ are isospin states (the same isospin states as for the nucleon, because both particles have isospin $1/2$), and $\tilde{\psi}_{Ri}$ is a radial phenomenological wave function depending on k and r . The functions X_ρ and X_λ are states which couple spin and orbital motion, and are respectively asymmetric and symmetric in the interchange of quarks (12). Since $l = 1$ is the angular momentum that is to be coupled with the core spin $1/2$ or $3/2$, the coupled orbital-spin states X_ρ and X_λ contain the spherical harmonics $Y_{1m}(r)$ and $Y_{1m}(k)$ ($m = 0, \pm$) coupled to the spin states of the three-quarks. It is convenient to write the spherical harmonics in terms of the spherical components of the three-momentum k and r . For instance for $Y_{1m}(k)$, one has $k_0 = k_z$, $k_\pm = \mp \frac{1}{\sqrt{2}}(k_x \pm ik_y)$, and we can write [6]

$$Y_{1m}(k) = \sqrt{\frac{3}{4\pi}} N_k k_m, \quad (4.8)$$

where $N_k = 1/|k|$, and \mathbf{k} is the diquark three-momentum. The form of the functions X_ρ and X_λ depends on the spin core state ($R1$ or $R3$), and their derivation is detailed in Appendices A and B.

Here we just briefly describe how to accommodate the needed internal $l = 1$ orbital angular momentum state of the diquark sub-structure (given by the $Y_{1m}(r)$ spherical harmonics that depends on the diquark internal relative momentum r). This is an important point because the inclusion of a diquark state with $l \neq 0$ implies that the diquark is not considered as pointlike particle (this was already encountered in the nucleon case [36] and we solve it here in the same fashion). To realize it, remember that because we are using impulse approximation, the internal variable r is integrated out, i.e., the full three-body wave function $\tilde{\psi}_R(r, k)$ is integrated in r . This integration is equivalent to averaging the full wave function in r and to generating an effective radial wave function corresponding to a quark-diquark structure, $\psi_R(P, k)$, that depends on the diquark momentum k only. Now, we may write $Y_{1m}(r)$ in terms of the spherical components of r , as in Eq. (4.8) with $k \rightarrow r$. That form exhibits the vector character of $Y_{1m}(r)$, and makes clear that the average over

the diquark internal states associated with $l = 1$ is not simply a scalar. Instead, after the full three-body wave function is averaged in r , the vector structure of $Y_{1m}(r)$ originates a polarization vector ζ_m^ν [36]. This new polarization vector is orthogonal to the diquark polarization vector $\varepsilon_{\Lambda P}^\alpha$, and satisfies

$$\sum_\nu \zeta_m^\nu \zeta_{m'}^{\nu*} = \delta_{mm'}. \quad (4.9)$$

The integration in the variable r amounts then to the replacement¹ [36]

$$Y_{1m}(r) \rightarrow c \zeta_m^\nu, \quad (4.10)$$

where we should set $c = 1$ in order to recover the result obtained when the explicit integration in r is performed, in the nonrelativistic limit. In addition, we replace also $\tilde{\psi}_R$ by ψ_R , where ψ_R is now a function of k only.

2. Relativistic generalization

The relativistic form of the wave function is obtained by extending the nonrelativistic quantities to their relativistic description. For example, since the nonrelativistic wave function was written in terms of the quark-diquark relative momentum $k = k_1 + k_2$, we have to construct the corresponding four-momentum. The general procedure involves the baryon momentum P , through the substitution $k \rightarrow \tilde{k}$ with

$$\tilde{k}^\alpha = k^\alpha - \frac{P \cdot k}{M_R^2} P^\alpha, \quad (4.11)$$

where P is the resonance momentum. In the rest frame of the resonance, $P = (M_R, 0, 0, 0)$, and $\tilde{k} = (0, \mathbf{k})$, and the formula above reduces to its three-dimensional components. The radial wave function $\tilde{\psi}_R$ will then be replaced by its relativistic form $\psi_R(P, k)$.

This procedure also helps us to establish the relativistic form for $Y_{1m}(k)$, by using Eq. (4.8). The replacement $k \rightarrow \tilde{k}$ defined by Eq. (4.11), extends the orbital angular momentum states from the rest frame to any frame, according to [6]

$$Y_{1m}(k) \rightarrow -N_{\tilde{k}} (\varepsilon_m \cdot \tilde{k}), \quad (4.12)$$

with $\varepsilon_m^\alpha \equiv \varepsilon_P^\alpha(m)$ and $N_{\tilde{k}} = \frac{1}{\sqrt{-\tilde{k}^2}}$.

The polarization states ζ_m^ν of Eq. (4.10) which will enter into the coupled spin-orbit states are also replaced by their relativistic generalization, normalized according to $\zeta_\Lambda \cdot \zeta_{\Lambda'}^* = -\delta_{\Lambda\Lambda'}$.

¹ In Ref. [36] a factor $|k|$ was included in the replacement (4.10), but that factor was canceled by a factor $1/|k|$ included in the radial wave function.

To finish the relativistic generalization we need to replace the two coupled orbital-spin coupled states, X_ρ and X_λ , by their full corresponding relativistic form. This is done in Appendices A and B, respectively for the $R1$ and $R3$ components of the wave function.

In Appendix A we obtain that the final expression for Ψ_{R1} is

$$\begin{aligned} \Psi_{R1}(P, k) = & \frac{1}{2} \left\{ (-\mathcal{T}_R \phi_I^0 + \phi_I^1) u_\zeta^\nu(P) \right. \\ & \left. - N_{\tilde{k}} (\phi_I^0 + \mathcal{T}_R \phi_I^1) \tilde{k}^\beta u_\beta(P) \right\} \psi_{R1}(P, k), \end{aligned} \quad (4.13)$$

where ψ_{R1} is a radial wave function,

$$u_\zeta^\nu(P, s) = \sum_{s'} \langle 1\frac{1}{2}; (s-s') s' | \frac{3}{2}s \rangle \zeta_{s-s'}^\nu u_R(P, s'), \quad (4.14)$$

with ζ_m^ν a spin-1 state introduced in Eq. (4.10), and

$$\mathcal{T}_R = \frac{1}{\sqrt{3}} (\varepsilon_{\Lambda P}^*)_\alpha \gamma_5 \left(\gamma^\alpha - \frac{P^\alpha}{M_R} \right). \quad (4.15)$$

It is relevant to interpret the meaning of each of the terms of Eq. (4.13). The terms in u_ζ^ν contain the states where the diquark is in an internal P -state (note the presence of ζ_m^ν in u_ζ^ν), while the terms in u_β contain the orbital quark-diquark P -state for the wave function (note \tilde{k}^β in the combination $\tilde{k}^\beta u_\beta$).

The terms in $u_\zeta^\nu(P)$ will not interfere with the nucleon wave function and have therefore no contribution to the transition current.

The radial wave function ψ_{R1} will be constrained in order to assure the orthogonality with the nucleon wave function as discussed below.

In Appendix B we obtain that the component $\Psi_{R3}(P, k)$ of the $N^*(1520)$ wave function is

$$\Psi_{R3}(P, k) = -\psi_{R3}(P, k) (\varepsilon_{\Lambda P}^*)^\beta (W_{R3})_\beta(P, s), \quad (4.16)$$

where ψ_{R3} is the radial wave function,

$$\begin{aligned} (W_{R3})_\beta(P, s) = & \frac{1}{\sqrt{2}} \gamma_5 \left[\phi_I^0 (V_\zeta^\nu)_\beta(P, s) - \phi_I^1 N_{\tilde{k}} \tilde{k}_\alpha (V_\varepsilon^\alpha)_\beta(P, s) \right], \end{aligned} \quad (4.17)$$

and

$$(V_\zeta^\nu)_\beta(P, s) = \sum_{s'} \langle 1\frac{3}{2}; (s-s') s' | \frac{3}{2}s \rangle \zeta_{s-s'}^\nu u_\beta(P, s') \quad (4.18)$$

$$(V_\varepsilon^\alpha)_\beta(P, s) = \sum_{s'} \langle 1\frac{3}{2}; (s-s') s' | \frac{3}{2}s \rangle \varepsilon_{s-s'}^\alpha u_\beta(P, s'). \quad (4.19)$$

In the equation for $(W_{R3})_\beta(P, s)$ the factor γ_5 gives the needed relativistic form for a state with negative parity.

Note in Eq. (4.17) that without the terms associated with the diquark internal P -states (the ones that contain

ζ^ν) only isospin-1 contributions remain, and therefore the charge of the state would differ from $\frac{1}{2}(1 + \tau_3)$. This shows that the diquark cannot be pointlike. Its internal structure, and particularly its $l = 1$ relative angular momentum has to be taken into account, since it plays an important role in the baryon properties.

C. Orthogonality conditions and the phenomenological radial functions

Within the quark-diquark picture of a baryon with total momentum P and diquark momentum k , the covariant spectator quark model wave function for a baryon includes, not only the spin-flavor structure, but also a radial function for the momentum distribution of the quark-diquark system. The forms for these functions are described in Appendix C.

In this work the radial baryon wave functions are not determined through a dynamical calculation, and are purely phenomenological. For the nucleon, the parameters were determined by the study of the nucleon form factors on Ref. [33] (model II). That parametrization was successfully applied to predict the transition form factors of the photo-excitation of the nucleon to other N^* 's.

The radial wave functions ψ_X ($X = N, R1, R3$) for the nucleon and the components of the wave function $N^*(1520)$ are normalized according to

$$\int_k |\psi_X(\bar{P}, k)|^2 = 1, \quad (4.20)$$

where \bar{P} is the baryon momentum at the rest frame. This condition correctly fixes the baryon charge. For instance, for the nucleon we obtain

$$3 \sum_\Gamma \int_k \bar{\Psi}_N(\bar{P}, k) j_1 \gamma^0 \Psi_N(\bar{P}, k) = e_N \left[\int_k |\psi_N(\bar{P}, k)|^2 \right], \quad (4.21)$$

where $j_1 \gamma^0$ is the quark charge operator, and $e_N = \frac{1}{2}(1 + \tau_3)$ is the nucleon charge. One realizes that the normalization condition (4.20) is required to obtain the right charge of the nucleon.

Another remark has to be done at this point. The wave function components in Eqs. (4.13) and (4.16) depend on the mass M_R of the system (for instance u_β , u_R and U_R^α depend on M_R). This implies that when the particles in the final and initial state have different masses their states are necessarily defined in different frames. Therefore, if no additional condition is imposed on the phenomenological radial function to enforce orthogonality, it becomes possible that states orthogonal in the nonrelativistic limit become not orthogonal in their relativistic generalization. An example found in previous studies was the $N^*(1535)$ state of negative parity [6]. The same happens here for the $N^*(1520)$ state.

We impose then the condition that the $R1$ and $R3$ components of the resonance wave function are orthogonal to

the nucleon wave function, i.e.,

$$3 \sum_{\Gamma} \int_k \bar{\Psi}_{Ri}(\bar{P}_+, k) j_1 \gamma^0 \Psi_N(\bar{P}_-, k) = 0, \quad (4.22)$$

when $Q^2 = 0$ (\bar{P}_+ and \bar{P}_- are the baryon momenta when $Q^2 = 0$). In particular in the resonance rest frame one has $\bar{P}_+ = (M_R, 0, 0, 0)$ and $\bar{P}_- = (E_N, 0, 0, -|\mathbf{q}|)$, where $E_N = \frac{M_R^2 + M^2}{2M_R}$ and $|\mathbf{q}| = \frac{M_R^2 - M^2}{2M_R}$. For the wave functions defined in this section Eq. (4.22) leads to

$$\int_k N_{\tilde{\mathbf{k}}}(\varepsilon_{0\bar{P}_+} \cdot \tilde{\mathbf{k}}) \psi_{Ri}(\bar{P}_+, k) \psi_N(\bar{P}_-, k) = 0. \quad (4.23)$$

This equation is used to fix the free parameters of the radial wave functions ψ_{R1} and ψ_{R3} respectively (see Appendix C). All the numerical values of the wave function parameters are given in Sec. VI where the numerical results are presented.

It is important to realize that the need to impose the orthogonality conditions (4.22) is a consequence of relativity. For $Q^2 = 0$, in the nonrelativistic limit there are no recoil effects, and therefore both particles are considered in their rest frames. In this limit then the overlap integral $\int_{\Omega_{\mathbf{k}}} Y_{10}(\hat{\mathbf{k}}) \psi_R \psi_N$, between the two baryon wave functions at $Q^2 = 0$, vanishes. In the relativistic case, however, because the nucleon and R have different masses, they cannot be simultaneously in their rest frame when $Q^2 = 0$. Then at least one of the wave functions is distorted by a boost, which induces a dependence on the direction of \mathbf{k} , and leads to $\int_{\Omega_{\mathbf{k}}} Y_{10}(\hat{\mathbf{k}}) \psi_R \psi_N \neq 0$.

V. TRANSITION FORM FACTORS

In this section we will present the algebraic results obtained for the transition form factors and helicity amplitudes from our quark core model. First, we will derive the separate contributions to the $\gamma N \rightarrow N^*(1520)$ transition form factors from the $R1$ and $R3$ components of the wave function.

Second, we will see that for small Q^2 we obtain amplitudes that are small when compared with the data. The reasons for this are identified. This result will give us an indication that meson cloud effects have to be considered, and therefore we finish this section by also giving a parametrization to describe them.

A. Quark core contributions

1. Contribution from the $R1$ -component

To calculate the the $R1$ -state contribution to the transition form factors we use the definition of the current (3.1), with Ψ_R given by Ψ_{R1} [see Eq. (4.13)]. Strictly speaking in Eq. (3.1) we should add the sum in the index ν to take into account the dependence on ζ^ν in the R

wave function. However, since those terms do not interfere with the nucleon wave function that is not necessary.

The details of the calculation are included in the Appendix D. The final results are

$$G_1^{R1} = -\frac{3}{2\sqrt{2}|\mathbf{q}|} \cos \theta_D \times \left[\left(j_1^A + \frac{1}{3} j_1^S \right) + \frac{M_R + M}{2M} \left(j_2^A + \frac{1}{3} j_2^S \right) \right] I_z^{R1} \quad (5.1)$$

$$G_2^{R1} = \frac{3}{2\sqrt{2}M|\mathbf{q}|} \cos \theta_D \times \left[j_2^A + \frac{1}{3} \frac{1 - 3\tau}{1 + \tau} j_2^S + \frac{4}{3} \frac{2M}{M_R + M} \frac{1}{1 + \tau} j_1^S \right] I_z^{R1} \quad (5.2)$$

$$G_3^{R1} = -\frac{3}{2\sqrt{2}|\mathbf{q}|} \frac{M_R - M}{Q^2} \cos \theta_D \times \left[j_1^A + \frac{1}{3} \frac{\tau - 3}{1 + \tau} j_1^S + \frac{4}{3} \frac{M_R + M}{2M} \frac{\tau}{1 + \tau} j_2^S \right] I_z^{R1}, \quad (5.3)$$

where $\tau = \frac{Q^2}{(M_R + M)^2}$,

$$I_z^{R1} = -\int_k N_{\tilde{\mathbf{k}}}(\varepsilon_{0P_+} \cdot \tilde{\mathbf{k}}) \psi_{R1}(P_+, k) \psi_N(P_-, k). \quad (5.4)$$

$j_i^S = \frac{1}{6} f_{i+} + \frac{1}{6} f_{i-} - \tau_3$ and $j_i^A = \frac{1}{6} f_{i+} - \frac{1}{2} f_{i-} - \tau_3$ with $i = 1, 2$.

In addition, one has

$$G_4^{R1} = 0. \quad (5.5)$$

From these results one can calculate G_M^{R1} and G_E^{R1} using Eqs. (2.12) and (2.13), as well as $A_{1/2}^{R1}$ and $A_{3/2}^{R1}$, using Eqs. (2.8) and (2.9). As $G_4^{R1} = 0$, we have

$$G_E^{R1} = -G_M^{R1}, \quad (5.6)$$

and consequently

$$A_{3/2}^{R1} = 0. \quad (5.7)$$

Therefore there is no contribution of the $R1$ component to $A_{3/2}$.

Equations (5.1)-(5.3) show the proportionality between the form factors and the overlap integral I_z^{R1} . For $Q^2 = 0$ one has $I_z^{R1}(0) = 0$ according to the orthogonality condition (4.23). The consequence is that $G_M^{R1}(0) = G_E^{R1}(0) = 0$ and $A_{1/2}^{R1}(0) = A_{3/2}^{R1}(0) = 0$. However, $G_C^{R1}(0)$ is not zero and is finite, according to Eqs. (2.11), (2.14) and (5.3), because $G_C^{R1} \propto I_z^{R1}/Q^2$ and by construction (through the orthogonality condition) $I_z^{R1} \propto Q^2$ when $Q^2 \rightarrow 0$.

2. Contribution from the $R3$ -component

The calculations of the contributions of the $R3$ component in the wave function to the transition form factors and the helicity amplitudes are detailed in Appendix E.

The results for the form factors are

$$G_M^{R3} = \frac{3}{\sqrt{5}} \mathcal{R} f_v I_z^{R3} \sin \theta_D \quad (5.8)$$

$$G_E^{R3} = 3G_M^{R3} = \frac{9}{\sqrt{5}} \mathcal{R} f_v I_z^{R3} \sin \theta_D \quad (5.9)$$

$$G_C^{R3} = 2\sqrt{\frac{2}{15}} I_z^{R3} \sin \theta_D \times \left(\frac{MM_R}{Q^2} j_1^S + \frac{M_R}{2(M_R - M)} j_2^S \right), \quad (5.10)$$

where we recall that $\mathcal{R} = \frac{1}{\sqrt{6}} \frac{M}{M_R - M}$,

$$f_v = j_1^S - \frac{M_R - M}{2M} j_2^S, \quad (5.11)$$

and

$$I_z^{R3} = - \int_k N_{\tilde{k}}(\varepsilon_{0P_+} \cdot \tilde{k}) \psi_{R3}(P_+, k) \psi_N(P_-, k). \quad (5.12)$$

The $R3$ -component contributions to $G_E(0)$ and $G_M(0)$ vanish because of the orthogonality condition between the initial and final states, i.e. $I_z^{R3}(0) = 0$. Only G_C is nonzero for $Q^2 = 0$, as it happened for the $R1$ -component.

The contribution from the $R3$ -state to G'_4 (which is proportional to $A_{3/2}$) is

$$(G'_4)^{R3} = -\frac{6}{\sqrt{5}} \mathcal{R} f_v I_z^{R3}. \quad (5.13)$$

For the helicity amplitudes one obtains

$$A_{3/2}^{R3} = -\frac{3}{\sqrt{5}} \sqrt{\frac{2\pi\alpha}{K}} N_q f_v I_z^{R3} \sin \theta_D, \quad (5.14)$$

$$A_{1/2}^{R3} = 0, \quad (5.15)$$

$$S_{1/2}^{R3} = \sqrt{\frac{2}{15}} \sqrt{\frac{2\pi\alpha}{K}} \bar{f}'_v N_q |\mathbf{q}| I_z^{R3} \sin \theta_D, \quad (5.16)$$

where

$$N_q = \sqrt{\frac{(M_R + M)^2 + Q^2}{4MM_R}}, \quad (5.17)$$

$$\bar{f}'_v = \frac{M_R - M}{Q^2} j_1^S + \frac{j_2^S}{2M}. \quad (5.18)$$

The helicity amplitudes and the form factors obtained from the $R3$ -component alone are proportional to $\sin \theta_D$, estimated to be ≈ 0.1 in some models [24]. For this reason we do not expect a significant effect from the $R3$ -component. It is nevertheless interesting to note that only this component gives a finite contribution to $A_{3/2}$. Although small, it could in principle be important to understand the falloff of the amplitude $A_{3/2}$ for large Q^2 . Also in contrast to the $R1$ -component, $R3$ does not contribute at all to $A_{1/2}$.

3. Summary and discussion of the quark core contributions

We can summarize the obtained results for the spin quark core contributions to the form factors in the following formulas (the index b stands for bare):

$$G_M^b = G_M^{R1} + G_M^{R3} \quad (5.19)$$

$$G_E^b = -G_M^{R1} + 3G_M^{R3} \quad (5.20)$$

$$G_C^b = G_C^{R1} + G_C^{R3}. \quad (5.21)$$

For G_4 only the $R3$ component of the wave function contributes:

$$(G'_4)^b = (G'_4)^{R3}. \quad (5.22)$$

Alternatively, for the helicity amplitudes, we have, following Eqs. (2.19)-(2.20) and (2.14):

$$A_{1/2}^b = \frac{1}{F} G_M^b + \frac{1}{4F} (G'_4)^b \quad (5.23)$$

$$A_{3/2}^b = \frac{\sqrt{3}}{4F} (G'_4)^b \quad (5.24)$$

$$S_{1/2}^b = \frac{\mathcal{K}}{F} G_C^b, \quad (5.25)$$

where $\mathcal{K} = \frac{1}{2\sqrt{2}} \frac{|\mathbf{q}|}{M_R}$.

Because the contributions from $R1$ are proportional to $\cos \theta_D \approx 0.99$, and the contributions from $R3$ are proportional to $\sin \theta_D \approx 0.11$, we can anticipate a small quark core contribution to $A_{3/2}$.

Using Eqs. (2.16) and (2.17) we conclude that, from the $R1$ contribution, $G_E = -G_M$ ($A_{3/2} = 0$), while from the $R3$ contribution, $G_E = 3G_M$ ($A_{1/2} = 0$). As the $R3$ admixture is small, we obtain $A_{3/2} \propto G'_4$ also small, and we can expect an almost correlation between G_E and G_M with $G_E \simeq -G_M$. In addition, only G_C has a non zero contribution for $Q^2 = 0$, from both $R1$ and $R3$ core spin states.

We may discuss a bit further these following general features of our results:

1. The reason why in our model the $R1$ state does not contribute to $A_{3/2}$, and consequently $A_{3/2} \approx 0$ for any Q^2 range, lies in the form of the $R1$ -state, and in particular in the specific structure of the diquark polarization vectors. In the fixed-axis representation [60] the diquark momentum is averaged along the direction of the reaction, defined by the three-momentum part of $\frac{1}{2}(P_+ + P_-)$. This is very successful to construct (orbital) angular momentum state components of the wave function, as shown for the nucleon and the Δ [4, 5, 33, 36]. However, it may happen that it is incomplete for the structure of the P -state excitations, in spite of the model being successful in the description of the state $N^*(1535)$ characterized also by P -state excitations [6].

2. Our result that the contribution from the $R1$ -component to the form factors G_M and G_E vanishes at $Q^2 = 0$ is consistent with a nonrelativistic framework: since the initial and final states have the same core spin ($S = 1/2$), they are necessarily orthogonal because of the orthogonality between spherical harmonics. In the relativistic case, since the initial and the final state have different masses, and the wave functions are defined in different frames, the boosts cannot be neglected and the orthogonality condition is not automatically satisfied. We are then forced to impose the orthogonality condition (4.23) between the initial and the final state — which gives at $Q^2 = 0$ a zero contribution to G_E and G_M , while making $G_C(0)$ finite. This form of imposing the orthogonality was already considered in the $\gamma^*N \rightarrow \Delta(1232)$ reaction and was there also responsible for the generation of nonzero and finite contributions to G_C [5]. In the case of $R3$ -component, the core spin state is different from the nucleon state ($S = 1/2$ for the nucleon and $S = 3/2$ for the $R3$ -component), and therefore $R3$ is also orthogonal to the nucleon wave function in the nonrelativistic limit. However as that does not happen in our relativistic generalization of the states for $N^*(1520)$, we are again forced to impose the orthogonality between the nucleon and the $R3$ -component.

3. In this work the nucleon wave function is reduced to an S -state configuration. It is possible that the states $R1$ and $R3$ interfere with nucleon P -states, as already proposed in Ref. [36]. Nevertheless, we expect those contributions to be small due to the small P -state admixture in the nucleon wave function.

B. Parametrization of the meson cloud

As explained already in the introduction, although our quarks are dressed, there are still meson cloud effects that can give extra contributions to the transition form factors. In general meson cloud contributions are expected to be significant at low Q^2 [1, 2]. It is then natural to assume that meson cloud effects can give important contributions for the helicity amplitudes at low Q^2 , in particular to the amplitude $A_{3/2}$, where our quark core model predicts only small contributions, because, as we have seen, the $R1$ -state contribution vanishes and the $R3$ -state is itself strongly suppressed by the weight factor $\sin\theta_D$. The small results of our model for $A_{3/2}$ are consistent with the conclusions of several authors [1, 2] and EBAC estimations [27] that the meson cloud effects for $A_{3/2}$ must be sizeable at least at low Q^2 .

Because the pion is the lightest meson, one may assume that pion cloud contributions dominate over heavier meson contributions, and also that heavy meson effects fall

off faster with Q^2 than pion effects. Another natural assumption on meson cloud effects is that diagrams where the photon couples with the meson in flight — the leading order contribution according to chiral perturbation theory [63–65], give larger contributions than diagrams where the photon couples with the whole baryon, while the meson in flight is dressing the baryon.

Assuming then that the meson cloud can be added to the core quark effects, and that the pion is the dominant contribution, we take the following structure for the form factors

$$G_M = G_M^b + G_M^\pi \quad (5.26)$$

$$G'_4 = (G'_4)^b + G_4^\pi \simeq G_4^\pi \quad (5.27)$$

$$G_C = G_C^b + G_C^\pi, \quad (5.28)$$

where G_M^π , G_4^π and G_C^π are the pion cloud contributions or the form factors, to be parametrized and extracted from the difference between the experimental data and the quark model results. The approximation in Eq. (5.27) corresponds to neglecting the $R3$ contributions. The impact of this approximation is small since the weight of $R3$ in the wave function is small.

From the previous relations we may write for G_E

$$\begin{aligned} G_E &\equiv -G_M - G'_4 \\ &\simeq -G_M^b - (G_M^\pi + G_4^\pi), \end{aligned} \quad (5.29)$$

and the helicity amplitudes become

$$A_{1/2} \simeq \frac{1}{F}G_M^b + \frac{1}{F}G_M^\pi + \frac{1}{4F}G_4^\pi \quad (5.30)$$

$$A_{3/2} \simeq \frac{\sqrt{3}}{4F}G_4^\pi \quad (5.31)$$

$$S_{1/2} = \frac{\mathcal{K}}{F}(G_C^b + G_C^\pi). \quad (5.32)$$

In the approximation of neglecting the $R3$ -state contributions, $A_{3/2}$ is reduced to the dominant G_4^π term. The fact that $A_{3/2}$ is only connected to G_4 , and does not mix other form factors is most fortunate, since then the meson cloud effect on G_4 can be directly read off from $A_{3/2}$ only. Similarly, the meson cloud effect on G_C can be separately read off from the $S_{1/2}$ data. Finally, the $A_{1/2}$ amplitude will mix that contribution with the contribution to G_4 . These results motivate the use of the helicity amplitudes data to breakdown the meson cloud effects into three independent terms, contributing respectively to G_4 , G_C , and finally G_M . The numerical results will be shown in the next section. The information on the three pion cloud terms was based on functional forms and inspired in previous studies of the pion cloud contribution in the timelike regime [50, 66].

The parametrization of the pion cloud contributions

that we use here is then

$$G_4^\pi = \lambda_\pi^{(4)} \left(\frac{\Lambda_4^2}{\Lambda_4^2 + Q^2} \right)^3 F_\rho \tau_3 \quad (5.33)$$

$$G_M^\pi = (1 + a_M Q^2) \times \lambda_\pi^M \left(\frac{\Lambda_M^2}{\Lambda_M^2 + Q^2} \right)^3 F_\rho \tau_3 \quad (5.34)$$

$$G_C^\pi = \lambda_\pi^C \left(\frac{\Lambda_C^2}{\Lambda_C^2 + Q^2} \right)^3 F_\rho \tau_3, \quad (5.35)$$

with

$$F_\rho = \frac{m_\rho^2}{m_\rho^2 + Q^2 + \frac{1}{\pi} \frac{\Gamma_\rho^0}{m_\pi} Q^2 \log \frac{Q^2}{m_\pi^2}}, \quad (5.36)$$

where m_ρ and m_π are the ρ and pion mass, and $\Gamma_\rho^0 = 0.149$ GeV [50]. The isospin operator τ_3 gives the isospin dependence of the diagram for the direct coupling between the photon and the pion [45, 63]. For the reaction starting with the proton the isospin dependence gives a + sign, while the neutron case brings in a - sign.

The adjustable parameters in the parametrization of the pion cloud are the strength coefficients $\lambda_\pi^{(4)}$, λ_π^M , λ_π^C and the cutoff parameters Λ_4 , Λ_M , Λ_C , as well as the coefficient a_M .

One important motivation for the forms from Eqs. (5.33)-(5.35) is the expected leading order behavior from pQCD: $G_M \propto 1/Q^4$, $G_4 \propto 1/Q^6$ and $G_C \propto 1/Q^6$ based in similar reactions [67, 68], corrected by an factor $1/Q^4$ due to the additional $q\bar{q}$ contribution, The extra factor $1/Q^4$ is a consequence of the estimation of the behavior of the leading order form factor G given by $G \propto 1/(Q^2)^{(N-1)}$, where N is the number of constituents, and comes from replacing $N = 3$ (3 quarks) by $N = 5$ (3 quarks + 1 quark-antiquark pair from the meson) [67]. In this work, the extra factor $1/Q^4$, due to the $q\bar{q}$ contribution, is slightly smoothed, and replaced by $F_\rho \propto 1/(Q^2 \log Q^2)$. See Ref. [50] for more details.

In the parametrization of G_M^π in Eq. (5.34), apart from the falloff with Q^2 of the simple multipole function, we included an extra term with a higher power dependence in Q^2 , when compared to the terms used for G_4^π and G_C^π . Different from the other form factor parametrizations, this term has no fundamental justification. It simply allows more flexibility in the phenomenological description of the pion cloud effects. While the function G_4^π that fixes $A_{3/2}$ and the function G_C^π that fixes $S_{1/2}$ have a simple falloff behavior, as we will see next in the graph for $A_{3/2}$ in Fig. 1, the pion cloud contributions to G_M require a more complex analytic form.

Note that although we adopt for simplicity a meson cloud parametrization with a structure corresponding to the pion cloud, we cannot exclude that it effectively contains contributions from heavier mesons, given the phenomenological fitting procedure.

VI. RESULTS

Here we present the numerical results of the covariant spectator quark model for the $\gamma^* N \rightarrow N^*(1520)$ reaction. We calculated the quark core model contributions to the helicity amplitudes and form factors, by applying the equations in Sec. V. First, we will compare our results to the experimental data, and in the sequel we will describe the difference between our quark core model contributions and the data by the meson cloud parametrization presented in the Sec. V B.

In the comparison to the data we use the PDG results for $Q^2 = 0$ [69] for the amplitudes $A_{1/2}$ and $A_{3/2}$, and the CLAS data for $Q^2 = 0.3 - 4.2$ GeV² [7] (pion production data) and for $Q^2 = 0.3 - 0.6$ GeV² [8] (double pion production data). At the end we also discuss and make predictions for the very large Q^2 region which may be measured after the Jlab 12-GeV upgrade.

A. Quark core effects

Our calculation of the quark core contributions includes the contributions from both $R1$ and $R3$, the quark core spin 1/2 and 3/2, respectively. As mentioned already, the first ones are proportional to $\cos \theta_D$ and the second ones proportional to $\sin \theta_D$. Because we are not using a dynamical model starting with a well defined quark-quark interaction, we cannot calculate θ_D , and we use then the most common estimation in the literature $\theta_D \simeq 6.3^\circ$ (with $\cos \theta_D \simeq 0.994$ and $\sin \theta_D = 0.110$) [14, 19, 24, 53].

In the following calculations we use the range parameters of the nucleon radial wave function (model II in Ref. [33]) defined by Eq. (C2). In particular we use $\beta_1 = 0.049$, $\beta_2 = 0.717$, corresponding to a normalization constant $N_0 = 3.35$.

We start with the results obtained with the $R1$ -state component only in the wave function. To test the sensitivity of the results to the radial wave function parametrization we consider first a model where the R radial wave function (ψ_{R1}) is taken to be identical to the nucleon radial wave function (ψ_N), written in terms of the R variables. Note that this model has no adjustable parameters. We label this model as model 0. The results are presented by the dashed lines, in Figs. 1 and 2, respectively for the helicity amplitudes and form factors. Because in this toy model the nucleon and R wave functions are not orthogonal in the relativistic formulation, it fails necessarily for low Q^2 , and therefore we plot the results only for $Q^2 > 1$ GeV².

It is interesting that the results from model 0 are very close to the data for $A_{1/2}$ and $S_{1/2}$. This suggests that the naive model gives a good first approximation to the R wave function, at least for high Q^2 . It means that in their inner core, probed in the high momentum transfer region, the baryons have a very similar structure. It also

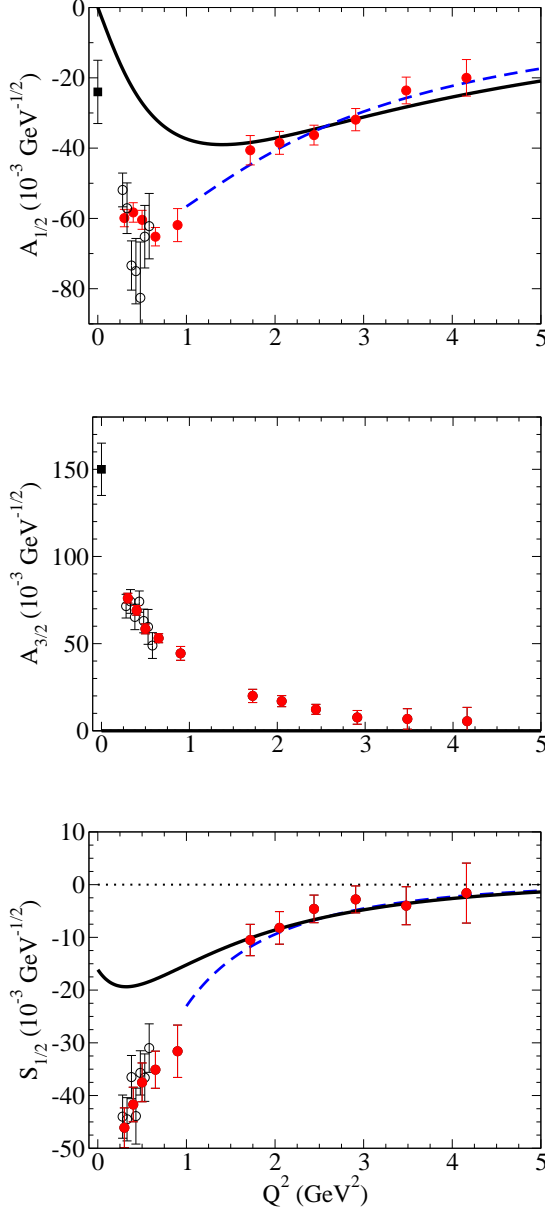


FIG. 1: Quark core contributions to the helicity amplitudes. The dashed line is the model 0. The solid line is the result from model 1 [fit of the parameter β_3 for $Q^2 > 1.5 \text{ GeV}^2$]. Data from Ref. [7] (full circles), Ref. [8] (empty circles) and PDG [69] (square).

means that in principle the toy model can be improved by re-adjusting the radial wave function.

We took therefore the radial wave function given by Eq. (C3), where a new range parameter β_3 can be chosen to obtain an improved description of the high Q^2 data, a region where the meson cloud effects are expected to be very small. The orthogonality with the nucleon state is then imposed using the Eq. (4.23). See the discussion in Sec. IV C. The parameter β_3 is determined by the fit to the data for $Q^2 > 1.5 \text{ GeV}^2$. The minimization of χ^2 , gives us $\beta_3 = 0.257$. The corresponding values for

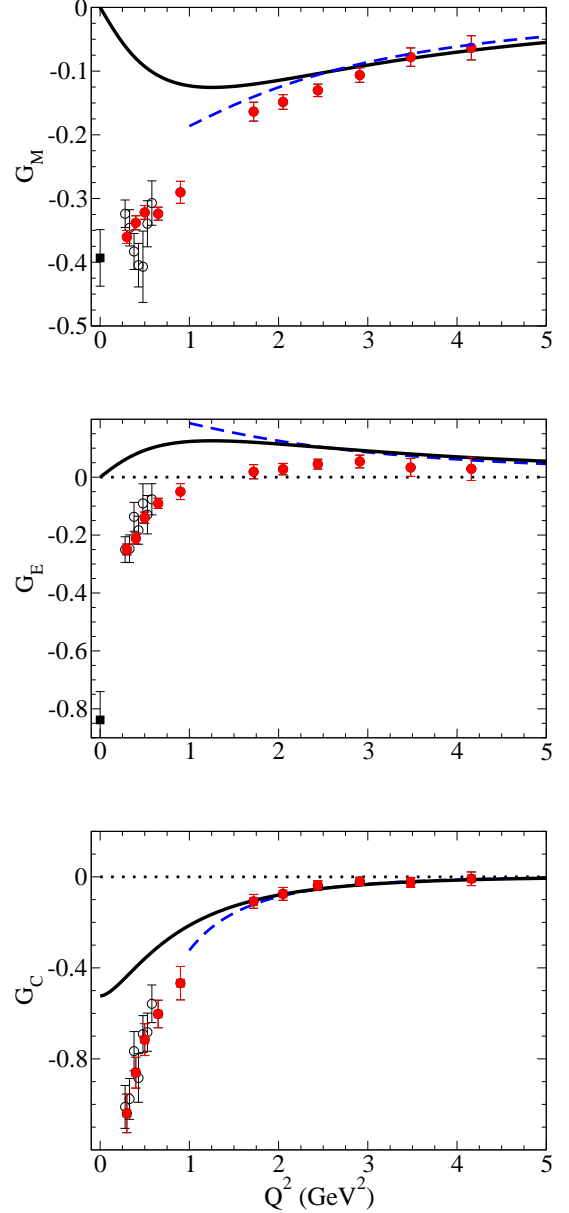


FIG. 2: Quark core contributions to the form factors. The dashed line is the model 0. The solid line is the result from model 1 [fit of the parameter β_3 for $Q^2 > 1.5 \text{ GeV}^2$]. Data from Ref. [7] (full circles), Ref. [8] (empty circles) and PDG [69] (square).

λ_{R1} and the normalization constant are $\lambda_{R1} = 0.519$ and $N_1 = 12.68$. We label this new model as model 1.

The results from model 1 for the helicity amplitudes in the resonance rest frame, and obtained with the $R1$ -state component only in the wave function, are presented in the Fig. 1. We conclude that the quark core contributions give a good description of the $A_{1/2}$ and $S_{1/2}$ data for $Q^2 > 1.5 \text{ GeV}^2$, but fail in the low Q^2 region for all the helicity amplitudes. These results justify our motivation to describe the low Q^2 region and the amplitude $A_{3/2}$ using an effective parametrization of the meson cloud ef-

a_M	$\lambda_\pi^{(4)}$	λ_π^M	λ_π^C
4.934	1.354	-0.404	-1.851
Λ_4^2	Λ_M^2	Λ_C^2	
20.0	1.663	1.850	

TABLE I: Model parameters for the pion cloud parametrization. a_M has units GeV^{-2} . The coefficients λ_π have no dimensions. The cutoffs are in units GeV^2 .

fects.

The results for the electromagnetic form factors are presented in Fig. 2. The same trend of the amplitudes is observed for the form factors, except that the discrepancy between the model and the data is larger for G_E . This happens because in this quark core model the amplitude $A_{3/2}$ is too small, and, according to Eq. (2.13) this amplitude has a relevant weight for G_E (3 times larger than the weight for G_M).

Next, we included the $R3$ -state in the resonance wave function. The contribution from this component was calculated using the radial wave function (C4) with the value $\alpha_1 = 0.337$ determined in Refs. [5, 40] for $\Delta(1232)$ (a resonance with core $S = 3/2$). Imposing that the $R3$ -state is orthogonal to the nucleon initial state, one obtains $\lambda_{R3} = 0.557$ and $N_3 = 7.16$. The results for the helicity amplitudes and form factors are presented in Fig. 3. The results are about 2 or 3 orders of magnitude smaller than the contributions from the $R1$ -state component. The main reason is the magnitude of the admixture coefficient, $\sin\theta_D \simeq 0.11$, but the smallness of the isospin coefficients $j_i^S = \frac{1}{6}(f_{i+} - f_{i-})$ also helps to suppress the $R3$ contributions. Note that $j_1^S(0) = 0$ and $j_2^S(0) = \frac{1}{6}(\kappa_+ - \kappa_-) \simeq 0.03$.

Figures 1 and 3 show that the $R1$ -state component dominates in the quark core effects. The smallness of the $R3$ -state contributions is the reason why we did not adjust a new range parameter to the corresponding radial function. The results from the full model are indeed not very sensitive to the $R3$ -state radial wave function.

B. Quark core and meson cloud effects combined

We have assumed that the decomposition given by Eqs. (5.30)-(5.32) is valid. Then we were able to use the parametrization from Eqs. (5.33)-(5.35) to describe the difference between the data and our quark core results – which we interpret as due to contributions from the meson cloud. We show now the results from combining the quark core effects with these meson cloud effects introduced in Sec. VB.

The parameters of the best fit are in Table I. We fit only the parameters related with the pion cloud dressing, since if we perform a combined fit of the valence plus pion cloud contributions we would lose control of the quark core content, and artificially very large pion cloud contributions emerge as numerical solutions. In

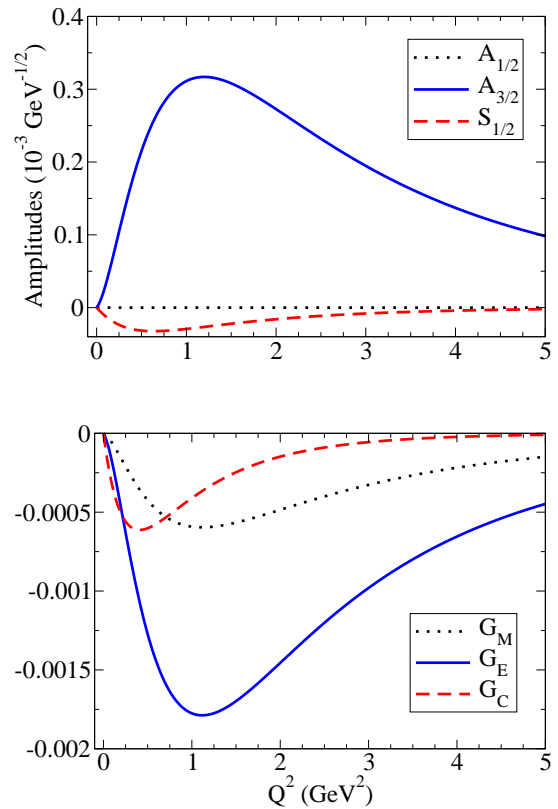


FIG. 3: Contributions from the state $R3$ to the amplitudes (at the top) and form factors (at the bottom). Note that those contributions are about 2 or 3 orders of magnitude smaller than the contributions from $R1$ or the experimental data (see Figs. 1 and 2).

this work we do not have an indirect way of calibrating the quark core contributions, as we did in our studies of the nucleon, Roper and the $\Delta(1232)$, where lattice QCD data are available [39, 40, 42]. The only way here to check that the quark core content is under control, is to extrapolate our model to the large Q^2 regime.

Concerning the fit, we note that the $A_{3/2}$ amplitude is determined only by the function G_4^π , but $A_{1/2}$ depends on both G_M^π and G_4^π . Nevertheless, an overall and simultaneous fit of the two amplitudes $A_{1/2}$ and $A_{3/2}$ (or G_4^π and G_M^π) is better constrained than the two-step procedure of fitting $A_{3/2}$ to fix separately G_4^π first, followed by an independent fit of $A_{1/2}$ to fix G_M^π . Finally, G_C^π is only constrained by the data from the amplitude $S_{1/2}$ (or form factor G_C).

In the fitting procedure we noticed that the best fit for $A_{3/2}$ is achieved when we fix the cutoff parameter Λ_4^2 in Eq. (5.33) at an extremely large value, such that the multipole factor in that formula behaves as a constant. To preserve a multipole falloff for very high Q^2 we took $\Lambda_4^2 = 20 \text{ GeV}^2$, allowing the multipole factor to behave like a constant in the Q^2 regime under study, although behaving as $1/Q^6$ for much larger values of Q^2 .

Using the parameters of the best fit (Table I) one can

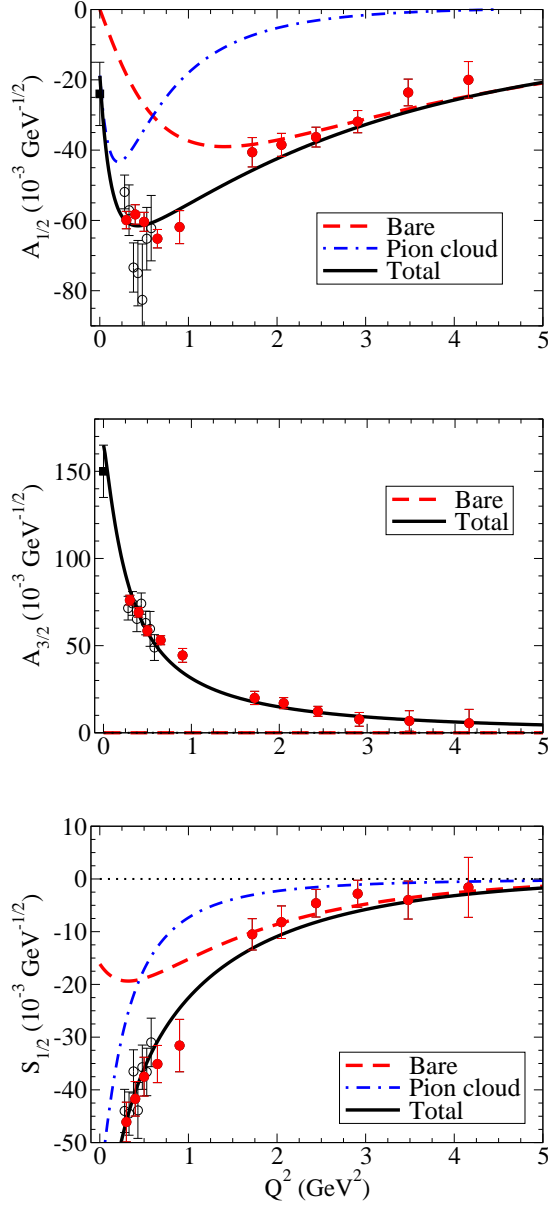


FIG. 4: Quark core plus pion cloud contributions to the helicity amplitudes. For the amplitude $A_{3/2}$ the pion cloud contribution coincides with the total. Data from Ref. [7] (full circles), Ref. [8] (empty circles) and PDG [69] (square).

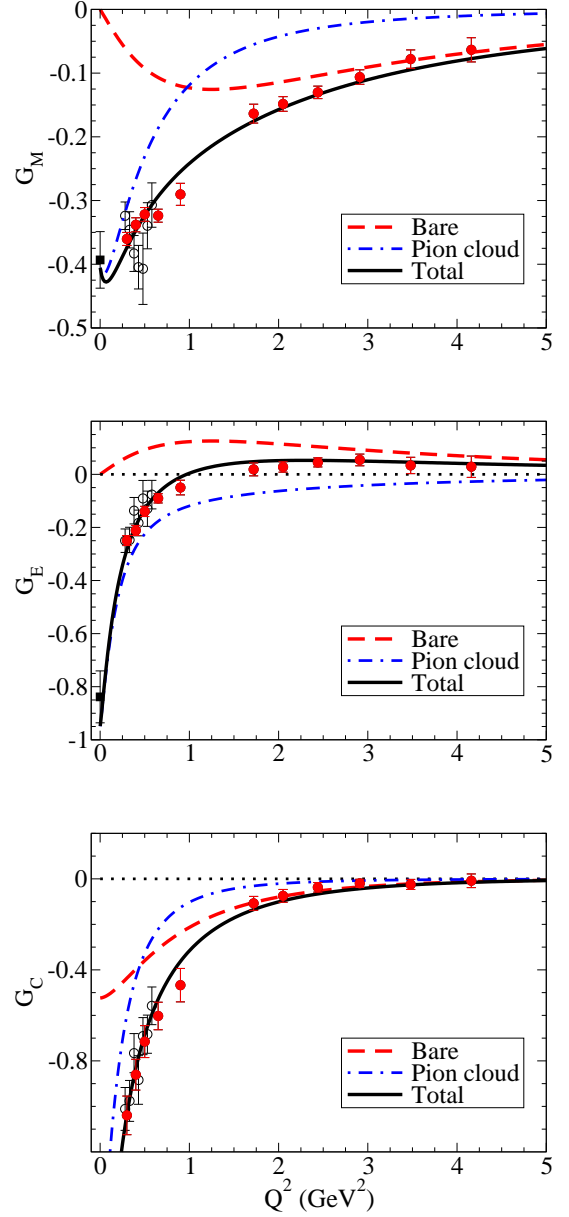


FIG. 5: Quark core plus pion cloud contributions to the form factors. Data from Ref. [7] (full circles), Ref. [8] (empty circles) and PDG [69] (square).

write the final form for the pion cloud contributions to

the helicity amplitudes as

$$A_{3/2}^\pi = 165 \sqrt{1 + \tau} \left(\frac{\Lambda_4^2}{\Lambda_4^2 + Q^2} \right)^3 F_\rho \tau_3 \quad (6.1)$$

$$A_{1/2}^\pi = -114 (1 + a_M Q^2) \sqrt{1 + \tau} \left(\frac{\Lambda_M^2}{\Lambda_M^2 + Q^2} \right)^3 F_\rho \tau_3 + \frac{1}{\sqrt{3}} A_{3/2}^\pi \quad (6.2)$$

$$S_{1/2}^\pi = -1094 \sqrt{1 + \frac{Q^2}{(M_R - M)^2}} \left(\frac{\Lambda_C^2}{\Lambda_C^2 + Q^2} \right)^3 F_\rho \tau_3. \quad (6.3)$$

Where the numerical coefficients are in units of $10^{-3} \text{ GeV}^{-1/2}$.

The results for the combination of the quark core and pion cloud contributions are presented in Fig. 4, for the helicity amplitudes, and in Fig. 5, for the form factors.

In Fig. 4, there is an excellent description of $A_{3/2}$, obtained with the parametrization of G_4^π . From the results for $A_{1/2}$ we conclude that the parametrization of the pion cloud for G_M^π is important to obtain a good description of the data at low Q^2 , and in particular, it is responsible for the minimum near $Q^2 \approx 0.2 \text{ GeV}^2$. It is this minimum that demands the inclusion of the factor $(1 + a_M Q^2)$ in the G_M^π parametrization. The shape of G_M^π is shown in the panel for G_M in Fig. 5. The results for the $S_{1/2}$ amplitude show that the pion cloud effects are large at low Q^2 [see Eq. (6.3)], but fall off very fast with Q^2 . In general, meson cloud effects explain well the low Q^2 behavior of all helicity amplitudes.

In Fig. 5 the form factor results encode the same information as the helicity amplitudes but in a different perspective. We can make two remarks on Fig. 5. Our first remark is the fast falloff of the pion cloud contributions to G_M and G_C . The second remark is that for G_E , the difference between the quark core contributions and the experimental data is still meaningful for $Q^2 > 2 \text{ GeV}^2$, and that the effect of the pion cloud comprises a significant fraction of the full result. This is a consequence of our results for $A_{3/2}$ being in great part determined by the pion cloud.

In the comparison of our work to the literature, our results agree with the general conclusion that at very high Q^2 the $A_{1/2}$ amplitude is the dominant helicity amplitude. This dominance of $A_{1/2}$ is equivalent to have in that regime $G_E \simeq -G_M$ [7, 13, 14]. [See Eqs. (2.12) and (2.13).] Our calculations are also consistent with the findings that in the low Q^2 regime the meson cloud contributions are decisive for the description of the data, as suggested by Ref. [27] within a coupled-channel formalism.

Compared to some estimations from constituent quark models [13–19], our model gives results for $A_{3/2}$ in the low Q^2 region that are too small. Although in Refs. [15–18, 21, 22], the result for $A_{3/2}$ near $Q^2 = 0$ is typically $1/3$ of the experimental result, Ref. [19] predicts a result

for $A_{3/2}(0)$ that is very close to the PDG value for small Q^2 . The possible explanations for our $A_{3/2} \approx 0$ result were already given in the discussion made in Sec. V A 3.

We may also compare our result for the form factor G_1 (or G_M [see Eq. (2.12)]) with the estimations of the light-front quark model from Ref. [20]. This model, contrary to our model, gives a good description of the $Q^2 < 1.5 \text{ GeV}^2$ data, even without meson cloud effects. But in that work, for the estimation of the effects of the meson cloud using high Q^2 data, the strength of the quark contributions was reduced about 20%. If we consider a similar reduction in our quark model we also improve our description of the data. Focusing on the graph for $A_{1/2}$ from Fig. 4 or the graph for G_M from Fig. 5, the suppression of 20% in the quark core contributions would shift our model results to be almost on top of the high Q^2 data, improving the result from the quark core contribution. Unfortunately, as our meson cloud estimation is phenomenological, and not determined together with the quark core wave function, we do not have a simple method to estimate the effect of the meson cloud in the normalization of our wave function. It is nevertheless encouraging to notice the convergence of the two different works.

C. Jlab and MAID parametrizations and extrapolation of our results to larger Q^2 values

Besides the CLAS analysis [7, 8] reported previously, there are also data from the MAID 2007 analysis, hereafter called MAID analysis. The results from MAID include the analysis from old data and recent Jlab data [29, 30].

In Ref. [1] a fit to the CLAS $A_{1/2}, A_{3/2}$ data based on rational functions of $Q = \sqrt{Q^2}$ was presented. We label it as Jlab parametrization. The MAID parametrization is a fit to the MAID analysis presented in Ref. [29], which instead is based on a combination of polynomials and exponentials of Q^2 . Because the MAID parametrization is dominated by exponential falloffs for large Q^2 , it does not reproduce the expected power law behavior from pQCD. The range of application of the MAID parametrization should then be restricted to the range of the available data.

The comparisons between the Jlab and MAID data, their parametrization fits and the results of the present model (labeled as Spectator) are shown in the panels of Fig. 6 for the helicity amplitudes. For the $S_{1/2}$ amplitude there is no Jlab parametrization. The two different parametrizations describe the respective data, but differ significantly. Note in particular for $A_{1/2}$ the difference of falloff between our model and the Jlab and MAID parametrizations when $Q^2 > 5 \text{ GeV}^2$. This makes extremely interesting the data for higher Q^2 values, possible by the forthcoming Jlab 12-GeV upgrade.

This is the reason why in this section we also look at the high Q^2 momentum transfer region, that may even-

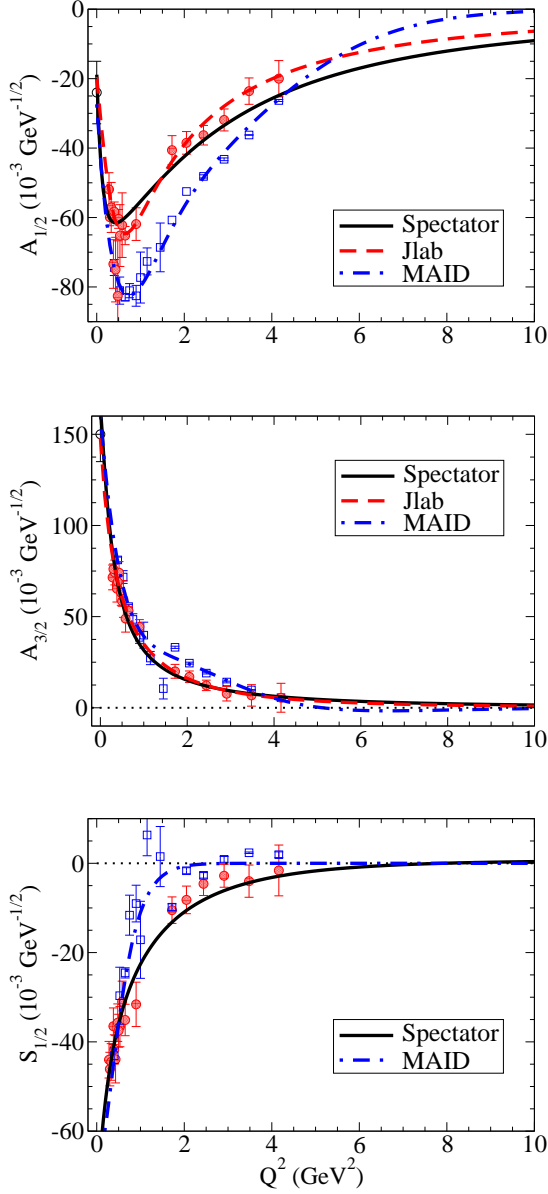


FIG. 6: Helicity amplitudes up to 10 GeV^2 . Comparing the spectator model with the CLAS data (circles) [7, 8] and the MAID analysis (squares) [29, 30]. The results of the Jlab [1] and MAID [29] parametrizations are also shown.

tually be explored with this upgrade. We extrapolated then our model to that region, and compared it with the Jlab and the MAID parametrizations, to predict when the scaling between G_M and G_E in that high Q^2 region appears. The different predictions for large Q^2 , in particular for $A_{1/2}$ and $A_{3/2}$, may be better analyzed by looking at the form factors G_M and G_E . This is because as the ratio $|A_{3/2}|/|A_{1/2}|$ falls off very quickly when Q^2 increases, it is expected that $-G_E$ approaches G_M in that regime. As both G_M and $-G_E$ fall off very fast with Q^2 , and assuming that G_M and G_E go with $1/Q^4$ for very large Q^2 , it is advantageous in the study of their asymp-

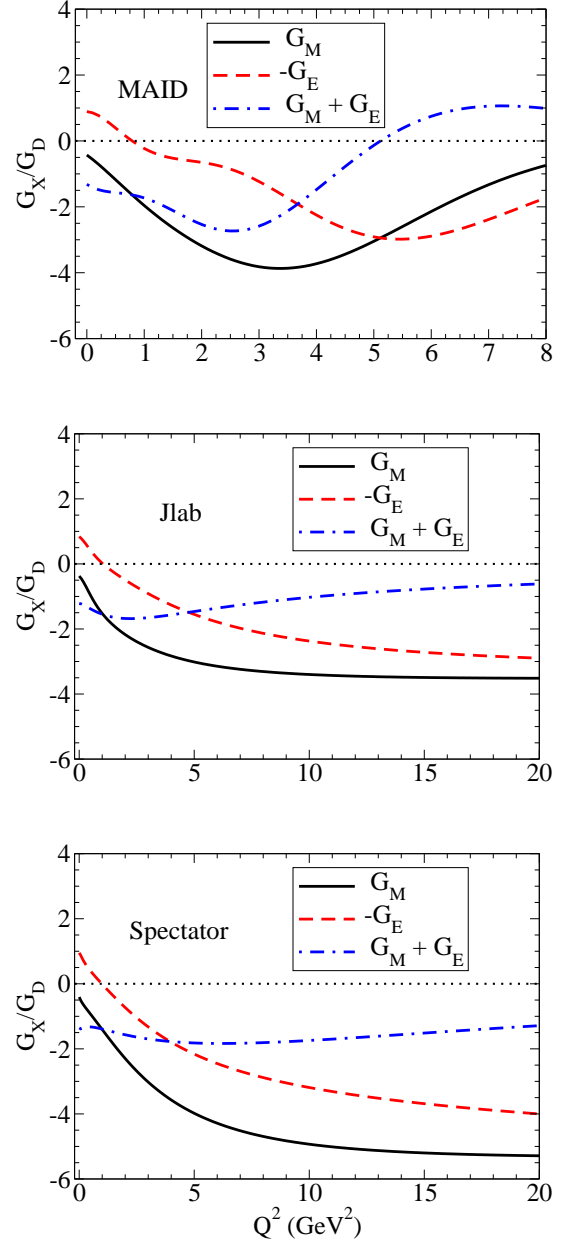


FIG. 7: Form factors, G_M , $-G_E$ and $G_M + G_E$ normalized by dipole form factor G_D given by Jlab [1] and MAID [29] parametrizations, and by the Spectator model.

totic behavior to normalize those form factors with the dipole form factor $G_D = \left(1 + \frac{Q^2}{0.71}\right)^{-2}$, with Q^2 given in GeV^2 . This enables a better visualization of the falloff tail and is usually done for the nucleon form factors. The results for, G_M , $-G_E$ and $G_M + G_E$, normalized by G_D , are presented in Fig. 7. It is interesting to look at the results for $G_M + G_E$, because pQCD predicts that it is strongly suppressed [67, 68].

In Fig. 7 we restrict the results from the MAID parametrization to the region $Q^2 < 8 \text{ GeV}^2$, due to the fast exponential falloff of the respective form factors. For

the Jlab parametrization of the data, and the Spectator model, we note the scaling of G_M and $-G_E$ with G_D , depicted by the almost flat lines obtained for $Q^2 > 15$ GeV², especially for G_M . In both cases we can observe also the falloff of $G_M + G_E$ with increasing Q^2 . Since $G_M + G_E$ is proportional to the amplitude $A_{3/2}$, the falloff of $G_M + G_E$ relative to G_M , is the sign of the suppression of $A_{3/2}$ relative to $A_{1/2}$.

Finally we note that in the large Q^2 region our model differs from the Jlab parametrization for G_M and $-G_E$: although our model and the data parametrization fall with the same $1/Q^4$ power, our results are larger in absolute value. That behavior can also be observed for $A_{1/2}$ in Fig. 6.

We conclude that future experiments, as the ones planned for the Jlab-12 GeV upgrade, will be crucial to better constrain models [2, 70].

VII. CONCLUSIONS

We have applied the covariant spectator quark model to the $N^*(1520)$ system and to the $\gamma^*N \rightarrow N^*(1520)$ reaction.

Our formulation takes the wave function of the $N^*(1520)$ as a combination of two components, $R1$ and $R3$, with core spin $1/2$ and $3/2$ respectively. We conclude that the model with only quark core effects included is particularly successful in the description of the high Q^2 data ($Q^2 > 2$ GeV²) of the $A_{1/2}$ and $S_{1/2}$ helicity amplitudes.

In the small Q^2 region there is a discrepancy between the data and our results for helicity amplitudes and form factors. This is not surprising since for small Q^2 the photon is expected to couple to the baryon as a whole and to the peripheral meson cloud, given the small momentum resolution (long wavelengths) of the electromagnetic probe.

As we do not include in our quark core model processes where the pion or heavier mesons collectively dress the three quarks, we have interpreted the deviations of our results from data in that region as meson cloud effects not present in our model, and we proceeded to obtain their parametrization.

The meson cloud parametrization used in the present work is inspired in previous parametrizations of pion cloud effects. However, since we obtain a good description of the overall data, it can be regarded as an effective representation of all meson cloud effects (including $\pi\pi N$ states).

In general we can say that our calculations are consistent with the data at relatively high Q^2 , the regime where the quark model is expected to work. Therefore, we also used our model to predict the observables in the high Q^2 region, projected to the Jlab 12-GeV upgrade. As other quark models, we predict that for large Q^2 : $G_E \simeq -G_M$, equivalent to the condition $|A_{1/2}| \gg |A_{3/2}|$, although

that asymptotic convergence is slow and $G_M + G_E$ is still significant at $Q^2 = 20$ GeV².

Our constituent quark model is restricted to a quark-diquark picture which may not include fully the orbital P -wave contributions to the resonance wave function. Nevertheless, this model describes the main features of the the $\gamma^*N \rightarrow N^*(1520)$ transition form factors, and the parametrizations obtained in this work may be very useful for the study of this reaction, particularly in the timelike regime [71].

Acknowledgments

This work was supported by the Brazilian Ministry of Science, Technology and Innovation (MCTI-Brazil), and Conselho Nacional de Desenvolvimento Científico e Tecnológico (CNPq), project 550026/2011-8. This work was supported also by Portuguese national funds through FCT – Fundação para a Ciência e a Tecnologia, under Grant No. PTDC/FIS/113940/2009, “Hadron Structure with Relativistic Models”, the project PEst-OE/FIS/UI0777/2011, and partially by the European Union under the HadronPhysics3 Grant No. 283286.

Appendix A: $R1$ -component

We start with the nonrelativistic form of the state Ψ_{R1} . Next we present the relativistic generalization.

1. Nonrelativistic wave function

For the case of the $R1$ component, for each total angular momentum projection, $s = \pm\frac{1}{2}, \pm\frac{3}{2}$ the orbital-spin states can be written as in Ref. [53]

$$\Psi_{R1}(s) = \frac{1}{2} [\phi_I^0 X_\rho + \phi_I^1 X_\lambda] \tilde{\psi}_{R1}, \quad (A1)$$

where

$$\begin{aligned} X_\rho(s) &= \sum_{ms'} \langle 1\frac{1}{2}; ms' | \frac{3}{2}s \rangle \left[Y_{1m}(k_\rho) |s'\rangle_\lambda + Y_{1m}(k_\lambda) |s'\rangle_\rho \right] \\ X_\lambda(s) &= \sum_{ms'} \langle 1\frac{1}{2}; ms' | \frac{3}{2}s \rangle \left[Y_{1m}(k_\rho) |s'\rangle_\rho - Y_{1m}(k_\lambda) |s'\rangle_\lambda \right], \end{aligned} \quad (A2)$$

and where the spin states $|s\rangle_\rho, |s\rangle_\lambda$:

$$|s\rangle_\rho = \sum_{s_1} \langle 0\frac{1}{2}; 0s_1 | \frac{1}{2}s \rangle \chi_{s_1} \equiv \chi_s \quad (A3)$$

$$|s\rangle_\lambda^i = \sum_{s_1} \langle 1\frac{1}{2}; 1s_1 | \frac{1}{2}s \rangle \epsilon_{s-s_1}^i \chi_{s_1}, \quad (A4)$$

for $s = \pm\frac{1}{2}$, are antisymmetric and symmetric, respectively, in the exchange of quarks 1 and 2. They are three-body coupled core spin states, $0 \oplus \frac{1}{2}$ and $1 \oplus \frac{1}{2}$ (labeled ρ

and λ), given in terms of the Pauli spinors χ_s , and defined respectively, as the axial-scalar and axial-vector diquark terms. The vector ϵ_m^i , (with Cartesian projections $i = 1, 2, 3$) is a spin-1 state and corresponds to the vector diquark. These spin states are normalized according to $\rho\langle s'|s\rangle_\rho = \delta_{s's}$, $\lambda^i\langle s'|s\rangle_\lambda^j = \frac{1}{3}\delta_{s's}\delta_{ij}$, $\sum_i \lambda^i\langle s'|s\rangle_\lambda^i = \delta_{s's}$ and $\rho\langle s'|s\rangle_\lambda = \lambda\langle s'|s\rangle_\rho = 0$.

We restrict the two momentum projections s to $s = +\frac{1}{2}, +\frac{3}{2}$ since symmetries relate the remaining cases to those. Therefore, with the notation $|\pm\rangle_\rho \equiv |\pm\frac{1}{2}\rangle_\rho$, $|\pm\rangle_\lambda \equiv |\pm\frac{1}{2}\rangle_\lambda$, we write

$$\begin{aligned} X_\rho(+\tfrac{1}{2}) &= +\frac{1}{\sqrt{3}} \left[Y_{1+1}(r)|-\rangle_\lambda + \sqrt{2}Y_{10}(r)|+\rangle_\lambda \right] \\ &\quad +\frac{1}{\sqrt{3}} \left[Y_{1+1}(k)|-\rangle_\rho + \sqrt{2}Y_{10}(k)|+\rangle_\rho \right] \\ X_\rho(+\tfrac{3}{2}) &= Y_{1+1}(r)|-\rangle_\lambda + Y_{1+1}(k)|-\rangle_\rho, \end{aligned} \quad (\text{A5})$$

and

$$\begin{aligned} X_\lambda(+\tfrac{1}{2}) &= +\frac{1}{\sqrt{3}} \left[Y_{1+1}(r)|-\rangle_\rho + \sqrt{2}Y_{10}(r)|+\rangle_\rho \right] \\ &\quad -\frac{1}{\sqrt{3}} \left[Y_{1+1}(k)|-\rangle_\lambda + \sqrt{2}Y_{10}(k)|+\rangle_\lambda \right] \\ X_\lambda(+\tfrac{3}{2}) &= Y_{1+1}(r)|+\rangle_\rho - Y_{1+1}(k)|+\rangle_\lambda. \end{aligned} \quad (\text{A6})$$

2. Relativistic generalization

We collect now all the prescriptions, namely Eqs. (4.10) and (4.12), to obtain the relativistic generalization the orbital-spin states $X_\rho(s)$ and $X_\lambda(s)$. In addition to those prescriptions the relativistic forms of $|s\rangle_\rho$ and $|s\rangle_\lambda$ are

$$\begin{aligned} |s\rangle_\rho &\rightarrow u_R(P, s) \\ |s\rangle_\lambda &\rightarrow -(\epsilon_P^*)_\alpha U_R^\alpha(P, s), \end{aligned} \quad (\text{A7})$$

where u_R is a Dirac spinor, and $U_R^\alpha(P, s)$ is given by Eq. (4.2). The procedure was used already in previous applications [6, 33, 36]. One has, collecting all the transformations:

$$\begin{aligned} X_\rho(+\tfrac{1}{2}) &= -\frac{1}{\sqrt{3}} \left[\zeta_+^\nu(\epsilon_{\Lambda P}^*)_\alpha U_R^\alpha(-) + \sqrt{2}\zeta_0^\nu(\epsilon_{\Lambda P}^*)_\alpha U_R^\alpha(+ \right] \\ &\quad -N_{\tilde{k}} \left[\frac{1}{\sqrt{3}}(\epsilon_- \cdot \tilde{k})u_R(-) + \sqrt{\frac{2}{3}}(\epsilon_0 \cdot \tilde{k})u_R(+ \right] \\ X_\rho(+\tfrac{3}{2}) &= -\zeta_+^\nu(\epsilon_{\Lambda P}^*)_\alpha U_R^\alpha(+) - N_{\tilde{k}}(\epsilon_+ \cdot \tilde{k})u_R(+), \end{aligned} \quad (\text{A8})$$

and

$$\begin{aligned} X_\lambda(+\tfrac{1}{2}) &= \frac{1}{\sqrt{3}} \left[\zeta_+^\nu u_R(-) + \sqrt{2}\zeta_0^\nu u_R(+ \right] \\ &\quad -N_{\tilde{k}} \left[\frac{1}{\sqrt{3}}(\epsilon_+ \cdot \tilde{k})(\epsilon_{\Lambda P}^*)_\alpha U_R^\alpha(-) + \sqrt{\frac{2}{3}}(\epsilon_0 \cdot \tilde{k})(\epsilon_{\Lambda P}^*)_\alpha U_R^\alpha(+ \right] \\ X_\lambda(+\tfrac{3}{2}) &= \zeta_+^\nu u_R(+) - N_{\tilde{k}}(\epsilon_+ \cdot \tilde{k})(\epsilon_P^*)_\alpha U_R^\alpha(+). \end{aligned} \quad (\text{A9})$$

Here, and in the following, for simplicity we adopt the notation $U_R^\alpha(\pm) \equiv U_R^\alpha(\pm\frac{1}{2})$, $u_R(\pm) \equiv u_R(\pm\frac{1}{2})$, and omit also the momentum P from the labeling of the spin states.

Finally, we may re-write these states in a short-hand notation by noting that the Rarita-Schwinger vector spin is, in the rest frame [4]

$$\begin{aligned} u^\beta(s) &= \sum_{s'} \langle 1\frac{1}{2}; (s-s') s' | \frac{3}{2}s \rangle \epsilon_{s-s'}^\beta u_R(s') \quad (\text{A10}) \\ &= \begin{cases} \epsilon_+^\beta u_R(+) & s = +\frac{3}{2} \\ \sqrt{\frac{2}{3}}\epsilon_0^\beta u_R(+) + \sqrt{\frac{1}{3}}\epsilon_+^\beta u_R(-) & s = +\frac{1}{2} \\ \sqrt{\frac{2}{3}}\epsilon_0^\beta u_R(-) + \sqrt{\frac{1}{3}}\epsilon_-^\beta u_R(+) & s = -\frac{1}{2} \\ \epsilon_-^\beta u_R(-) & s = -\frac{3}{2} \end{cases}, \end{aligned}$$

using the state $u_\zeta^\nu(s')$ defined by Eq. (4.14), and

$$\mathcal{T}_R = \frac{1}{\sqrt{3}}(\epsilon_P^*)_\alpha \gamma_5 \left(\gamma^\alpha - \frac{P^\alpha}{M_R} \right). \quad (\text{A11})$$

We obtain then

$$X_\rho(s) = -\mathcal{T}_R u_\zeta^\nu(s) + N_{\tilde{k}} \tilde{k}^\beta u_\beta(s) \quad (\text{A12})$$

$$X_\lambda(s) = u_\zeta^\nu(s) - N_{\tilde{k}} \mathcal{T}_R \tilde{k}^\beta u_\beta(s). \quad (\text{A13})$$

Finally we can write the $R1$ -state relativistic wave function as

$$\begin{aligned} \Psi_{R1}(s) &= N_{R1} \left\{ (-\mathcal{T}_R \phi_I^0 + \phi_I^1) u_\zeta^\nu(s) \right. \\ &\quad \left. - N_{\tilde{k}} (\phi_I^0 + \mathcal{T}_R \phi_I^1) \tilde{k}^\beta u_\beta(s) \right\} \psi_{R1}(P, k), \end{aligned} \quad (\text{A14})$$

where ψ_{R1} generalizes the function $\tilde{\psi}_{R1}$. The constant N_{R1} was introduced by convenience and is related to the function ψ_{R1} .

If we want to suppress the diquarks with internal P -states (pointlike diquark limit), we should remove the terms in u_ζ^ν .

By construction the wave function Ψ_{R1} is a solution of the Dirac equation: $\mathcal{P}\Psi_{R1} = M_R\Psi_{R1}$.

3. Normalization

The relativistic wave function, as the nonrelativistic one, is normalized by the charge condition

$$\begin{aligned} Q &= \sum_{\nu\Gamma} \int_k \Psi_{R1}^\dagger(\bar{P}, k) (3j_1) \Psi_{R1}(\bar{P}, k), \\ &= \frac{1}{2}(1 + \tau_3), \end{aligned} \quad (\text{A15})$$

defined at $Q^2 = 0$ for $\bar{P} = (M_R, 0, 0, 0)$. Note the inclusion of the index ν in order to take into account the contributions of the P -state diquarks. Using the previous definition, we obtain

$$Q = 6(j_1^A + j_1^S) N_{R1}^2 \int_k |\psi_{R1}(\bar{P}, k)|^2, \quad (\text{A16})$$

with j_1^A and j_1^S defined by Eqs. (D3)-(D4) for $Q^2 = 0$. As $3(j_1^A + j_1^S) = (1 + \tau_3)$, and imposing

$$\int_k |\psi_{R1}(\bar{P}, k)|^2 = 1, \quad (\text{A17})$$

we obtain the condition $N_{R1}^2 = 1/4$, or

$$N_{R1} = \frac{1}{2}. \quad (\text{A18})$$

We recover then the nonrelativistic normalization given by Eq. (A1).

Note however that if we suppress the diquarks with internal P -states one obtain instead $N = 1/\sqrt{2}$. That was the option considered in the study of the $\gamma^* N \rightarrow N^*(1535)$ reaction [6].

Appendix B: $R3$ -component

The $R3$ component of the $N^*(1520)$ wave function, which corresponds to core spin $3/2$, in the nonrelativistic framework, is defined as the coupled configuration $1 \oplus \frac{3}{2} \rightarrow \frac{3}{2}$. One can write then [53]

$$\Psi_{R3}(s) = \frac{1}{\sqrt{2}} [\phi_I^0 X_\rho(s) + \phi_I^1 X_\lambda(s)] \tilde{\psi}_{R3}, \quad (\text{B1})$$

where $\tilde{\psi}_{R3} = \tilde{\psi}_{R3}(r, k)$, and now

$$X_\rho(s) = \sum_{ms'} \langle 1\frac{3}{2}; ms' | \frac{3}{2}s \rangle Y_{1m}(r) \chi_{s'}^S, \quad (\text{B2})$$

$$X_\lambda(s) = \sum_{ms'} \langle 1\frac{3}{2}; ms' | \frac{3}{2}s \rangle Y_{1m}(k) \chi_{s'}^S, \quad (\text{B3})$$

where $\chi_{s'}^S$ is the totally symmetric spin state.

To obtain the relativistic extension of the wave function $R3$ component, we apply the replacements for the spherical harmonics (4.10), (4.12) and the relativistic generalization of $\chi_{s'}^S$ given in terms of the Rarita-Schwinger vector spin u_β

$$\chi_s^S \rightarrow -(\varepsilon_{\Lambda P}^*)^\beta u_\beta(P, s). \quad (\text{B4})$$

With everything together, the relativistic wave function becomes the expression given by Eqs. (4.16)-(4.17). The last step was the replacement $\tilde{\psi}_{R3} \rightarrow \psi_{R3}(P, k)$.

The wave function (4.16) is normalized using the charge condition equivalent to (A15), with

$$\int_k |\psi_{R3}(\bar{P}, k)|^2 = 1, \quad (\text{B5})$$

and leads us to the factor $1/\sqrt{2}$, in Eq. (4.17), identical to the nonrelativistic case [53] given by Eq. (B1).

The state Ψ_{R3} has the property $\not{P}\Psi_{R3} = -M_R\Psi_{R3}$. The $-$ sign is a consequence of the factor γ_5 in Eq. (4.17), which contrasts with the state $R1$.

Appendix C: Phenomenological radial functions

The phenomenological radial functions that are part of the baryon wave functions are written in terms of the scalar quantity $P \cdot k$. More specifically, they are written as functions of the dimensionless variable χ which in the nonrelativistic limit becomes proportional to \mathbf{k}^2 , and is defined as

$$\chi_B = \frac{(M_B - m_D)^2 - (P - k)^2}{M_B m_D}. \quad (\text{C1})$$

In this formula M_B is the baryon mass (M for the nucleon or M_R for the excited state).

The nucleon radial wave function is [33]

$$\psi_N(P, k) = \frac{N_0}{m_D(\beta_1 + \chi_N)(\beta_2 + \chi_N)}, \quad (\text{C2})$$

where β_1, β_2 are two momentum range parameters and N_0 is a normalization constant. If $\beta_2 > \beta_1$, β_2 regulates the short range behavior and β_1 the long range behavior in configuration space.

For the $R1$ -state component we use

$$\psi_{R1}(P, k) = \frac{N_1}{m_D(\beta_2 + \chi_R)} \left[\frac{1}{(\beta_1 + \chi_R)} - \frac{\lambda_{R1}}{(\beta_3 + \chi_R)} \right], \quad (\text{C3})$$

where N_1 is a normalization constant, β_3 is a new (short range) parameter, and λ_{R1} will be determined by the orthogonality condition (4.23) between the nucleon and that component of the N^* wave function.

For the state $R3$ we choose also a form with two terms, but with a parametrization similar to the one used in another work for the radial wave function of the $\Delta(1232)$ [40] in the S -state. It reads

$$\psi_{R3}(P, k) = \frac{N_3}{m_D(\alpha_1 + \chi_R)^3} \left(1 - \frac{\lambda_{R3}}{\alpha_1 + \chi_R} \right), \quad (\text{C4})$$

where N_3 is a normalization constant, α_1 is the momentum range, taken to be the same as the one of the $\Delta(1232)$ case, and λ_{R3} a coefficient to be determined also by the orthogonality condition (4.23).

At the moment then we introduce in our model only one more range parameter (β_3) to add to the already calibrated range parameters of the nucleon radial wave function.

Appendix D: Transition current — $R1$ component

Using the expressions given for the nucleon and Ψ_{R1} wave functions, we can calculate the transition current in relativistic impulse approximation [33, 34, 36]

$$J_{NR}^\mu \equiv 3 \sum_{\Gamma} \int_k \bar{\Psi}_{R1}(P_+, k) j_q^\mu \Psi_N(P_-, k). \quad (\text{D1})$$

Recall that

$$j_q^\mu = j_1 \hat{\gamma}^\mu + j_2 \mathcal{O}^\mu, \quad (\text{D2})$$

where $\mathcal{O}^\mu = \frac{i\sigma^{\mu\nu}q_\nu}{2M}$.

To work the spin algebra we project the quark current j_q^μ into the isospin states defining the coefficients

$$j_i^A = (\phi_I^0)^\dagger j_i \phi_I^0 = j_i \quad (\text{D3})$$

$$\begin{aligned} j_i^S &= (\phi_I^1)^\dagger j_i \phi_I^1 = \frac{1}{3} \tau_j j_i \tau_j \\ &= \frac{1}{6} f_{i+} - \frac{1}{6} f_{i-} \tau_3. \end{aligned} \quad (\text{D4})$$

In both cases we include the effect of the diquark polarization in the transition. This is done by summing the initial and final polarization vectors, and one obtains [4, 60]:

$$\begin{aligned} \Delta^{\alpha\beta} &\equiv \sum_\Lambda (\varepsilon_{\Lambda P_+})^\alpha (\varepsilon_{\Lambda P_-}^*)^\beta \\ &= - \left(g^{\alpha\beta} - \frac{P_-^\alpha P_+^\beta}{x} \right) \\ &\quad - a \left(P_- - \frac{x}{M_R^2} P_+ \right)^\alpha \left(P_+ - \frac{x}{M^2} P_- \right)^\beta \end{aligned} \quad (\text{D5})$$

where $x = P_+ \cdot P_-$, and

$$a = \frac{MM_R}{x[MM_R + x]}. \quad (\text{D6})$$

As the states Ψ_{R1} and Ψ_N are solutions of the Dirac equation and the asymptotic states are on-mass-shell we can simplify the operators $\hat{\gamma}^\mu$ and \mathcal{O}^μ to

$$\begin{aligned} \hat{\gamma}^\mu &\rightarrow \gamma^\mu - \frac{M_R - M}{q^2} q^\mu \\ \mathcal{O}^\mu &\rightarrow \frac{M_R + M}{2M} \gamma^\mu - \frac{P^\mu}{M}, \end{aligned} \quad (\text{D7})$$

recalling that $P = \frac{1}{2}(P_+ + P_-)$.

The direct calculation gives

$$\begin{aligned} \sum_\Lambda \bar{\Psi}_{R1} (3j_q^\mu) \Psi_N &= \mathcal{A} \left[\bar{u}_\beta \tilde{k}^\beta \{ j_1^A \hat{\gamma}^\mu + j_2^A \mathcal{O}^\mu \} u \right. \\ &\quad - \frac{1}{3} \bar{u}_\beta \tilde{k}^\beta \{ j_1^S \gamma^\alpha \hat{\gamma}^\mu \gamma^\sigma \Delta_{\alpha\sigma} \} u \\ &\quad \left. + \frac{1}{3} \bar{u}_\beta \tilde{k}^\beta \{ j_2^S \gamma^\alpha \tilde{\mathcal{O}}^\mu \gamma^\sigma \Delta_{\alpha\sigma} \} u \right], \end{aligned} \quad (\text{D8})$$

where $\Delta_{\alpha\sigma}$ is defined by Eq. (D5), $\mathcal{A} = -\frac{3N_{\tilde{k}}}{\sqrt{2}} \psi_{R1} \psi_N$, $\tilde{\mathcal{O}}^\mu = \gamma_5 \mathcal{O}^\mu \gamma_5$, and j_i^A and j_i^S defined by Eqs. (D3) and (D4) include the effect of the isospin. In the derivation (D8) we take advantage also of the relations $P_+^\alpha \Delta_{\alpha\sigma} = \Delta_{\alpha\sigma} P_-^\sigma = 0$.

We reduce therefore the calculation of the transition current J_{NR}^μ to the calculation of $\gamma^\alpha \hat{\gamma}^\mu \gamma^\sigma \Delta_{\alpha\sigma}$ and $\gamma^\alpha \tilde{\mathcal{O}}^\mu \gamma^\sigma \Delta_{\alpha\sigma}$, where

$$\tilde{\mathcal{O}}^\mu \rightarrow -\frac{M_R + M}{2M} \gamma^\mu - \frac{P^\mu}{M}. \quad (\text{D9})$$

We start calculating

$$\begin{aligned} \gamma^\alpha \gamma^\sigma \Delta_{\alpha\sigma} &= -3 \\ \gamma^\alpha \gamma^\mu \gamma^\sigma \Delta_{\alpha\sigma} &= -\gamma^\mu + 4A(M_R + M)P^\mu \\ &\quad - 2A(M_R - M)q^\mu, \end{aligned} \quad (\text{D10})$$

where $A = \frac{2}{(M_R + M)^2 + Q^2}$. The previous relations are valid when projected in the states $\bar{u}_\beta(P_+)$ and $u(P_-)$.

Using Eqs. (D10) we derive

$$\begin{aligned} \gamma^\alpha \hat{\gamma}^\mu \gamma^\sigma \Delta_{\alpha\sigma} &= -\hat{\gamma}^\mu + 4A(M_R + M) \left(P^\mu - \frac{P \cdot q}{q^2} q^\mu \right) \\ &= -\gamma^\mu + 4A(M_R + M)P^\mu + B \frac{M_R - M}{q^2} q^\mu, \end{aligned} \quad (\text{D11})$$

$$\begin{aligned} \gamma^\alpha \tilde{\mathcal{O}}^\mu \gamma^\sigma \Delta_{\alpha\sigma} &= \frac{M_R + M}{2M} \gamma^\mu + [3 - 2A(M_R + M)^2] \frac{P^\mu}{M} \\ &\quad + A \frac{M_R + M}{M} (M_R - M) q^\mu, \end{aligned} \quad (\text{D12})$$

where $B = -\frac{3(M_R + M)^2 - Q^2}{(M_R + M)^2 + Q^2}$. The relations (D11) and (D12) are valid between asymptotic states.

With the relations (D7), (D11) and (D12) we can represent (D8) as

$$\sum_\Lambda \bar{\Psi}_{R1} (3j_q^\mu) \Psi_N = \mathcal{A} \bar{u}_\beta \tilde{k}^\beta [g_1 \gamma^\mu + g_2 P^\mu + g_3 q^\mu] u, \quad (\text{D13})$$

where

$$\begin{aligned} g_1 &= \left(j_1^A + \frac{1}{3} j_1^S \right) + \frac{M_R + M}{2M} \left(j_2^A + \frac{1}{3} j_2^S \right) \quad (\text{D14}) \\ g_2 &= -\frac{1}{M} \left[j_2^A + \frac{1}{3} \frac{1 - 3\tau}{1 + \tau} j_2^S + \frac{4}{3} \frac{2M}{M_R + M} \frac{1}{1 + \tau} j_1^S \right] \end{aligned} \quad (\text{D15})$$

$$\begin{aligned} g_3 &= \frac{M_R - M}{Q^2} \times \\ &\quad \left[j_1^A + \frac{1}{3} \frac{\tau - 3}{1 + \tau} j_1^S + \frac{4}{3} \frac{M_R + M}{2M} \frac{\tau}{1 + \tau} j_2^S \right], \end{aligned} \quad (\text{D16})$$

with $\tau = \frac{Q^2}{(M_R + M)^2}$.

We can now calculate the current J_{NR}^μ given by Eq. (D1), performing the integration in k :

$$J_{NR}^\mu = -\frac{3N}{\sqrt{2}} \mathcal{I}^\beta \bar{u}_\beta \{ g_1 \gamma^\mu + g_2 P^\mu + g_3 q^\mu \} u, \quad (\text{D17})$$

where

$$\mathcal{I}^\beta = \int_k \tilde{k}^\beta N_{\tilde{k}} \psi_{R1}(P_+, k) \psi_N(P_-, k). \quad (\text{D18})$$

The previous integral is covariant, therefore the result is frame independent. We can write \mathcal{I}^β in a covariant form as

$$\mathcal{I}^\beta = \frac{\tilde{q}^\beta}{|\mathbf{q}|} I_z^{R1} \quad (\text{D19})$$

where $\tilde{q}^\beta = q^\beta - \frac{P \cdot q}{M_R^2} P^\beta$, $|\mathbf{q}| = \sqrt{-\tilde{q}^2}$ is an invariant, and

$$I_z^{R1} = - \int_k N_{\tilde{k}} (\varepsilon_0 \cdot \tilde{k}) \psi_{R1}(P_+, k) \psi_N(P_-, k), \quad (\text{D20})$$

is an invariant scalar function. In the resonance R rest frame one has the simple form

$$I_z^{R1} = \int_k \frac{k_z}{|\mathbf{k}|} \psi_{R1}(P_+, k) \psi_N(P_-, k), \quad (\text{D21})$$

where $P_+ = (M_R, 0, 0, 0)$ and $P_- = (E_N, 0, 0, -|\mathbf{q}|)$, with $E_N = \frac{M_R^2 + M^2 + Q^2}{2M_R}$ and $|\mathbf{q}|$ is given by Eq. (2.4).

Combining Eq. (D17) with (D19) we can write

$$J_{NR}^\mu = \bar{u}_\beta(P_+) \{G_1 q^\beta \gamma^\mu + G_2 q^\beta P^\mu + G_3 q^\beta q^\mu\} u(P_-), \quad (\text{D22})$$

where

$$G_i = - \frac{3N}{\sqrt{2}} \frac{I_z^{R1}}{|\mathbf{q}|} g_i, \quad (\text{D23})$$

for $i = 1, 2, 3$. As there is no term in $g^{\beta\mu}$, we conclude that

$$G_4 = 0. \quad (\text{D24})$$

As the contribution of the $R1$ -state in the $N^*(1520)$ wave function from Eq. (4.4) is proportional to $\cos \theta_D$, the helicity amplitudes and the form factors are affected by the same weight.

Appendix E: Transition current — $R3$ component

Instead of considering the general expression for the current (3.1), as for the $R1$ -state, we will use in this case the definition of the helicity amplitudes (2.2)-(2.3), at the resonance rest frame. Later we can use Eqs. (2.9)-(2.10) to extract the form factors. The main reason for this procedure is that the components of the $R3$ -state are not now written in terms of the Rarita-Schwinger states but there are more coefficients involved [see Eqs. (4.16)-(4.19)].

To calculate the helicity amplitudes we start with the current (3.1):

$$J_{NR}^\mu(s', s) = \sum_\Lambda \bar{\Psi}_{R3}(P_+, k; s') (3j_q^\mu) \Psi_N(P_-, k; s), \quad (\text{E1})$$

where the spin projections are explicitly included. The sum symbol includes only the diquark polarization index (Λ) because only the isovector components of the wave functions contribute. Next we consider the projection with the photon polarization vector $\epsilon_+(q)$ and $\epsilon_0(q)$, not to be confused with the diquark polarization vectors $\varepsilon_{\Lambda P}$. The calculations can be simplified using the Gordon decomposition for the quark current, taking advantage of the relation $P_- \Psi_N = M \psi_N$ and that $P_+ \Psi_{R3} = -M_R \Psi_{R3}$ to obtain the simplification

$$j_q^\mu \rightarrow \left(j_1 - \frac{M_R - M}{2M} j_2 \right) \gamma^\mu - j_2 \frac{P^\mu}{M} - \frac{M_R + M}{Q^2} j_1 q^\mu, \quad (\text{E2})$$

where we recall that $P = \frac{1}{2}(P_+ + P_-)$. We note that the calculations can be further reduced since $q \cdot \epsilon_{0,+} = 0$ and $P \cdot \epsilon_+ = 0$. Therefore we will use j_- to represent the effective term

$$j_- = j_1 - \frac{M_R - M}{2M} j_2. \quad (\text{E3})$$

Summing in the (isovector) isospin states we obtain

$$\begin{aligned} f_v &= (\phi_I^1)^\dagger j_- (\phi_I^1) \\ &= j_1^S - \frac{M_R - M}{2M} j_2^S, \end{aligned} \quad (\text{E4})$$

using the notation from Eq. (D4).

As for the state $R1$ -state one can separate the dependence in the radial wave function into the covariant function

$$I_z^{R3} = - \int_k N_{\tilde{k}} (\varepsilon_{0P_+} \cdot \tilde{k}) \psi_{R3}(P_+, k) \psi_N(P_-, k). \quad (\text{E5})$$

The final calculation requires the use of the Dirac spinors for the final state, $P_+ = (M_R, 0, 0, 0)$

$$u_R(s') = \begin{bmatrix} 1 \\ 0 \end{bmatrix} \chi_{s'}, \quad (\text{E6})$$

and for the initial state, $P_- = (E_N, 0, 0, -|\mathbf{q}|)$:

$$u(s) = N_q \begin{bmatrix} 1 \\ -|\tilde{q}| \end{bmatrix} \chi_s, \quad (\text{E7})$$

where $N_q = \sqrt{\frac{E_N + M}{2M}}$ and $|\tilde{q}| = \frac{|\mathbf{q}|}{M + E_N}$. The expressions for the final states are necessary because at the resonance rest frame we can represent the Rarita-Schwinger states in terms of the Dirac spinors using Eq. (A10).

For future reference we write N_q in a covariant form

$$N_q = \sqrt{\frac{(M_R + M)^2 + Q^2}{4MM_R}}. \quad (\text{E8})$$

1. Amplitude $A_{3/2}$

Considering the definition (2.1) and the procedures described previously, one can write, using the wave functions $\Psi_{R3}(P_+, k; +\frac{3}{2})$ and $\Psi_N(P_-, k; +\frac{1}{2})$

$$A_{3/2} = -\frac{3}{2}\sqrt{\frac{2\pi\alpha}{K}}Cf_v I_z^{R3} T_{3/2}, \quad (\text{E9})$$

where $C = \langle 1\frac{3}{2}; 0 + \frac{3}{2} | \frac{3}{2} + \frac{3}{2} \rangle = \sqrt{\frac{3}{5}}$, and

$$T_{3/2} = -\frac{1}{\sqrt{3}} [\bar{u}_\beta (+\frac{3}{2}) \gamma^\mu (\epsilon_+)_\mu \gamma_\alpha u (+\frac{1}{2})] \Delta^{\beta\alpha}. \quad (\text{E10})$$

Using the property $q^\beta \bar{u}_\beta (+\frac{3}{2}) = 0$, we can reduce the previous expression to

$$T_{3/2} = -\frac{2}{\sqrt{3}} N_q. \quad (\text{E11})$$

The final expression for the amplitude is then

$$A_{3/2} = \frac{3}{\sqrt{5}} \sqrt{\frac{2\pi\alpha}{K}} N_q f_v I_z^{R3}. \quad (\text{E12})$$

The corresponding expression for G_4 , given by Eq. (2.9), is

$$G_4 = \frac{3}{\sqrt{5}} f_v I_z^{R3}. \quad (\text{E13})$$

2. Amplitude $A_{1/2}$

We start with the expression (2.2) and use the wave functions $\Psi_{R3}(P_+, k; +\frac{1}{2})$ and $\Psi_N(P_-, k; -\frac{1}{2})$. Based in the previous discussion we reduce the calculation to

$$A_{1/2} = -\frac{3}{2}\sqrt{\frac{2\pi\alpha}{K}}Cf_v I_z^{R3} T_{1/2}, \quad (\text{E14})$$

where $C = \langle 1\frac{1}{2}; 0 + \frac{1}{2} | \frac{3}{2} + \frac{1}{2} \rangle$, and

$$T_{1/2} = -\frac{1}{\sqrt{3}} [\bar{u}_\beta (+\frac{1}{2}) \gamma^\mu (\epsilon_+)_\mu \gamma_\alpha u (+\frac{1}{2})] \Delta^{\beta\alpha}. \quad (\text{E15})$$

Using the expression

$$\bar{u}_\beta (+\frac{1}{2}) = \sqrt{\frac{3}{2}} \bar{u}_R (+\frac{1}{2}) (\epsilon_0^*)_\beta + \sqrt{\frac{3}{2}} \bar{u}_R (-\frac{1}{2}) (\epsilon_+^*)_\beta, \quad (\text{E16})$$

we can continue with the calculation, using the results $\epsilon_0^* \cdot \epsilon_+ = 0$, $\epsilon_+^* \cdot \epsilon_+ = -1$, $\epsilon_+^* \cdot q = 0$ and $\epsilon_0^* \cdot q = -|\mathbf{q}|$. One obtains then

$$T_{1/2} = \frac{2}{3} [\bar{u}_R (-\frac{1}{2}) u (+\frac{1}{2})] = 0. \quad (\text{E17})$$

The final result is a consequence of the orthogonality of the states $u_R(-\frac{1}{2})$ and $u(+\frac{1}{2}) = 0$.

In conclusion

$$A_{1/2} = 0. \quad (\text{E18})$$

Because $A_{3/2} = 0$, we can write $G_E = 3G_M$ and $A_{3/2} = -\frac{\sqrt{3}}{F} G_M$ [see Eqs. (2.16)-(2.17)].

3. Amplitude $S_{1/2}$

We consider now the amplitude $S_{1/2}$, as defined by Eq. (2.3), using the wave functions $\Psi_{R3}(P_+, k; +\frac{1}{2})$ and $\Psi_N(P_-, k; +\frac{1}{2})$. We start noting that when the current conservation is assured, as in the present case, we can replace $(\epsilon_0 \cdot J_{NR}) \frac{|\mathbf{q}|}{Q}$ by J_{NR}^0 , defined by Eq. (2.5) with J_{NR}^μ replaced by J_{NR}^0 .

We start with the calculation of the matrix element at the R rest frame

$$J_{NR}^0 = \sum_\Lambda \int_k \bar{\Psi}_{R3}(P_+, k; +\frac{1}{2}) (3j'_-) \Psi_N(P_-, k; +\frac{1}{2}), \quad (\text{E19})$$

where

$$j'_- = \left(1 - \frac{M_R + M}{Q^2} q^0\right) j_1 \gamma^0 - \left(\frac{P^0}{M} + \frac{M_R - M}{2M}\right) j_2, \quad (\text{E20})$$

as derived from Eq. (E2).

We can simplify the calculation using the relation $\bar{\Psi}_{R3}(P_+, k, s') \gamma^0 = \bar{\Psi}_{R3}(P_+, k, s') \frac{P_+}{M_R} = -\bar{\Psi}_{R3}(P_+, k, s')$, valid at the rest frame. The components P^0 and q^0 refer to the R rest frame

$$P^0 = \frac{3M_R^2 + M^2 + Q^2}{4M_R} \quad (\text{E21})$$

$$q^0 = \frac{M_R^2 - M^2 - Q^2}{2M_R}. \quad (\text{E22})$$

In that case Eq. (E19) is still valid with

$$\begin{aligned} j'_- &\rightarrow -j'_- \\ &= -\left(1 - \frac{M_R + M}{Q^2} q^0\right) j_1 - \left(\frac{P^0}{M} + \frac{M_R - M}{2M}\right) j_2. \end{aligned} \quad (\text{E23})$$

Taking in consideration the isospin effect, one has

$$\begin{aligned} f'_v &= (\phi_I^1)^\dagger j'_- (\phi_I^1) \\ &= \frac{(M_R + M)^2 + Q^2}{2M_R} \left[\frac{M_R - M}{Q^2} j_1^S + \frac{j_2^S}{2M} \right]. \end{aligned} \quad (\text{E24})$$

In these conditions we can write

$$S_{1/2} = -\frac{3}{2}\sqrt{\frac{2\pi\alpha}{K}} C f'_v I_z^{R3} T_0, \quad (\text{E25})$$

where $C = \langle 1\frac{1}{2}; 0 + \frac{1}{2} | \frac{3}{2} + \frac{1}{2} \rangle = \frac{1}{\sqrt{15}}$, and

$$T_0 = \frac{1}{\sqrt{3}} [\bar{u}_\beta (+\frac{1}{2}) \gamma_\alpha u (+\frac{1}{2})] \Delta^{\beta\alpha}. \quad (\text{E26})$$

The explicit calculation gives

$$T_0 = \frac{4\sqrt{2}}{3} \frac{M_R |\mathbf{q}|}{(M_R + M)^2 + Q^2} N_q. \quad (\text{E27})$$

At the end we obtain

$$S_{1/2} = -\sqrt{\frac{2}{15}} \sqrt{\frac{2\pi\alpha}{K}} N_q |\mathbf{q}| \bar{f}'_v I_z^{R3}, \quad (\text{E28})$$

where

$$\begin{aligned} \bar{f}'_v &= \frac{2M_R}{(M_R + M)^2 + Q^2} f'_v \\ &= \frac{M_R - M}{Q^2} j_1^S + \frac{j_2^S}{2M}. \end{aligned} \quad (\text{E29})$$

As for G_C , one has

$$G_C = -2\sqrt{\frac{2}{15}} \left(\frac{MM_R}{Q^2} j_1^S + \frac{M_R}{2(M_R - M)} j_2^S \right) I_z^{R3}. \quad (\text{E30})$$

Because the contribution of the $R3$ -state in the $N^*(1520)$ wave function from Eq. (4.4) is proportional to $-\sin\theta_D$, the helicity amplitudes and the form factors are affected by the same weight.

-
- [1] I. G. Aznauryan and V. D. Burkert, *Prog. Part. Nucl. Phys.* **67**, 1 (2012) [arXiv:1109.1720 [hep-ph]].
- [2] I. G. Aznauryan, A. Bashir, V. Braun, S. J. Brodsky, V. D. Burkert, L. Chang, C. Chen and B. El-Bennich *et al.*, *Int. J. Mod. Phys. E* **22**, 1330015 (2013) [arXiv:1212.4891 [nucl-th]].
- [3] V. Pascalutsa, M. Vanderhaeghen and S. N. Yang, *Phys. Rept.* **437**, 125 (2007) [hep-ph/0609004].
- [4] G. Ramalho, M. T. Peña and F. Gross, *Eur. Phys. J. A* **36**, 329 (2008) [arXiv:0803.3034 [hep-ph]].
- [5] G. Ramalho, M. T. Peña and F. Gross, *Phys. Rev. D* **78**, 114017 (2008) [arXiv:0810.4126 [hep-ph]].
- [6] G. Ramalho and M. T. Peña, *Phys. Rev. D* **84**, 033007 (2011) [arXiv:1105.2223 [hep-ph]].
- [7] I. G. Aznauryan *et al.* [CLAS Collaboration], *Phys. Rev. C* **80**, 055203 (2009) [arXiv:0909.2349 [nucl-ex]].
- [8] V. I. Mokeev *et al.* [CLAS Collaboration], *Phys. Rev. C* **86**, 035203 (2012) [arXiv:1205.3948 [nucl-ex]].
- [9] A. Faessler, C. Fuchs, M. I. Krivoruchenko, and B. V. Martemyanov, *J. Phys. G* **29**, 603 (2003) [nucl-th/0010056].
- [10] L. P. Kaptari and B. Kampfer, *Phys. Rev. C* **80**, 064003 (2009) [arXiv:0903.2466 [nucl-th]].
- [11] J. Weil, H. van Hees, and U. Mosel, *Eur. Phys. J. A* **48**, 111 (2012) [Erratum-ibid. *A* **48**, 150 (2012)] [arXiv:1203.3557 [nucl-th]].
- [12] G. Agakishiev, A. Balanda, D. Belder, A. Belyaev, J. C. Berger-Chen, A. Blanco, M. Bmer and J. L. Boyard *et al.*, arXiv:1403.3054 [nucl-ex].
- [13] F. E. Close and F. J. Gilman, *Phys. Lett. B* **38**, 541 (1972).
- [14] R. Koniuk and N. Isgur, *Phys. Rev. D* **21**, 1868 (1980) [Erratum-ibid. *D* **23**, 818 (1981)].
- [15] M. Warns, W. Pfeil and H. Rollnik, *Phys. Rev. D* **42**, 2215 (1990).
- [16] M. Aiello, M. M. Giannini and E. Santopinto, *J. Phys. G* **24**, 753 (1998) [nucl-th/9801013].
- [17] D. Merten, U. Loring, K. Kretzschmar, B. Metsch and H. R. Petry, *Eur. Phys. J. A* **14**, 477 (2002) [hep-ph/0204024].
- [18] E. Santopinto and M. M. Giannini, *Phys. Rev. C* **86**, 065202 (2012).
- [19] S. Capstick and B. D. Keister, *Phys. Rev. D* **51**, 3598 (1995) [nucl-th/9411016].
- [20] I. G. Aznauryan and V. D. Burkert, *Phys. Rev. C* **85**, 055202 (2012) [arXiv:1201.5759 [hep-ph]].
- [21] M. Ronniger and B. C. Metsch, *Eur. Phys. J. A* **49**, 8 (2013) [*Eur. Phys. J. A* **49**, 8 (2013)] [arXiv:1207.2640 [hep-ph]].
- [22] B. Golli and S. Sirca, *Eur. Phys. J. A* **49**, 111 (2013) [arXiv:1306.3330 [nucl-th]].
- [23] F. E. Close, *An Introduction To Quarks And Partons*, (Academic Press, London 1979)
- [24] V. D. Burkert, R. De Vita, M. Battaglieri, M. Ripani and V. Mokeev, *Phys. Rev. C* **67**, 035204 (2003) [hep-ph/0212108].
- [25] V. D. Burkert and T. S. H. Lee, *Int. J. Mod. Phys. E* **13**, 1035 (2004) [nucl-ex/0407020].
- [26] R. Bijker, F. Iachello and A. Leviatan, *Phys. Rev. C* **54**, 1935 (1996) [nucl-th/9510001].
- [27] B. Julia-Diaz, T. S. H. Lee, A. Matsuyama, T. Sato and L. C. Smith, *Phys. Rev. C* **77**, 045205 (2008) [arXiv:0712.2283 [nucl-th]].
- [28] L. Tiator, D. Drechsel, S. S. Kamalov and M. Vanderhaeghen, *Eur. Phys. J. ST* **198**, 141 (2011) [arXiv:1109.6745 [nucl-th]].
- [29] L. Tiator, D. Drechsel, S. S. Kamalov and M. Vanderhaeghen, *Chin. Phys. C* **33**, 1069 (2009) [arXiv:0909.2335 [nucl-th]].
- [30] D. Drechsel, S. S. Kamalov and L. Tiator, *Eur. Phys. J. A* **34**, 69 (2007) [arXiv:0710.0306 [nucl-th]].
- [31] R. Haidan, DESY-F21-79/03 (unpublished) J. -C. Alder, F. W. Brasse, W. Fehrenbach, J. Gayler, S. P. Goel, R. Haidan, V. Korbel and J. May *et al.*, *Nucl. Phys. B* **105**, 253 (1976); J. -C. Alder, F. W. Brasse, W. Fehrenbach, J. Gayler, R. Haidan, G. Glo, S. P. Goel and V. Korbel *et al.*, *Nucl. Phys. B* **91**, 386 (1975).
- [32] W. J. Shuttleworth, A. Sofair, R. Siddle, B. Dickinson, M. Ibbotson, R. Lawson, H. E. Montgomery and R. D. Hellings *et al.*, *Nucl. Phys. B* **45**, 428 (1972); E. Evangelides, R. Meaburn, J. Allison, B. Dickinson, M. Ibbotson, R. Lawson, H. E. Montgomery and D. Baxter *et al.*, *Nucl. Phys. B* **71**, 381 (1974); A. Latham, J. Allison, I. Booth, B. Dickinson, S. R. Hill, M. Ibbotson, R. Lawson and H. E. Mills *et al.*, *Nucl. Phys. B* **189**, 1 (1981).

- [33] F. Gross, G. Ramalho and M. T. Peña, Phys. Rev. C **77**, 015202 (2008) [nucl-th/0606029].
- [34] G. Ramalho, K. Tsushima and F. Gross, Phys. Rev. D **80**, 033004 (2009) [arXiv:0907.1060 [hep-ph]].
- [35] G. Ramalho, F. Gross, M. T. Peña and K. Tsushima, in *Proceedings of the 4th Workshop on Exclusive Reactions at High Momentum Transfer, 2011*, edited by A. Radyushkin (World Scientific, Singapore, 2011) p. 287 [arXiv:1008.0371 [hep-ph]].
- [36] F. Gross, G. Ramalho and M. T. Peña, Phys. Rev. D **85**, 093005 (2012) [arXiv:1201.6336 [hep-ph]].
- [37] F. Gross, G. Ramalho and M. T. Peña, Phys. Rev. D **85**, 093006 (2012) [arXiv:1201.6337 [hep-ph]].
- [38] F. Gross, Phys. Rev. **186**, 1448 (1969); J. W. Van Orden, N. Devine and F. Gross, Phys. Rev. Lett. **75**, 4369 (1995); A. Stadler, F. Gross and M. Frank, Phys. Rev. C **56**, 2396 (1997). [arXiv:nucl-th/9703043].
- [39] G. Ramalho and M. T. Peña, J. Phys. G **36**, 115011 (2009) [arXiv:0812.0187 [hep-ph]].
- [40] G. Ramalho and M. T. Peña, Phys. Rev. D **80** (2009) 013008 [arXiv:0901.4310 [hep-ph]].
- [41] G. Ramalho, M. T. Peña and F. Gross, Phys. Rev. D **81**, 113011 (2010) [arXiv:1002.4170 [hep-ph]]; G. Ramalho, M. T. Peña and A. Stadler, Phys. Rev. D **86**, 093022 (2012) [arXiv:1207.4392 [nucl-th]].
- [42] G. Ramalho and K. Tsushima, Phys. Rev. D **81** (2010) 074020 [arXiv:1002.3386 [hep-ph]].
- [43] G. Ramalho and K. Tsushima, Phys. Rev. D **84**, 051301 (2011) [arXiv:1105.2484 [hep-ph]].
- [44] G. Ramalho and K. Tsushima, Phys. Rev. D **82**, 073007 (2010) [arXiv:1008.3822 [hep-ph]].
- [45] F. Gross, G. Ramalho and K. Tsushima, Phys. Lett. B **690**, 183 (2010) [arXiv:0910.2171 [hep-ph]].
- [46] G. Ramalho and K. Tsushima, Phys. Rev. D **84**, 054014 (2011) [arXiv:1107.1791 [hep-ph]].
- [47] G. Ramalho, K. Tsushima and A. W. Thomas, J. Phys. G **40**, 015102 (2013) [arXiv:1206.2207 [hep-ph]].
- [48] G. Ramalho, D. Jido and K. Tsushima, Phys. Rev. D **85**, 093014 (2012) [arXiv:1202.2299 [hep-ph]]; G. Ramalho and K. Tsushima, Phys. Rev. D **86**, 114030 (2012) [arXiv:1210.7465 [hep-ph]]; G. Ramalho and K. Tsushima, Phys. Rev. D **88**, 053002 (2013) [arXiv:1307.6840 [hep-ph]]; G. Ramalho and M. T. Peña, Phys. Rev. D **83**, 054011 (2011) [arXiv:1012.2168 [hep-ph]].
- [49] G. Ramalho and K. Tsushima, Phys. Rev. D **87**, 093011 (2013) [arXiv:1302.6889 [hep-ph]].
- [50] G. Ramalho and M. T. Peña, Phys. Rev. D **85**, 113014 (2012) [arXiv:1205.2575 [hep-ph]].
- [51] B. Julia-Diaz, T. -S. H. Lee, T. Sato and L. C. Smith, Phys. Rev. C **75**, 015205 (2007) [nucl-th/0611033].
- [52] G. Eichmann and D. Nicmorus, Phys. Rev. D **85**, 093004 (2012) [arXiv:1112.2232 [hep-ph]].
- [53] S. Capstick and W. Roberts, Prog. Part. Nucl. Phys. **45**, S241 (2000) [nucl-th/0008028].
- [54] H. F. Jones and M. D. Scadron, Annals Phys. **81**, 1 (1973).
- [55] R. C. E. Devenish, T. S. Eizenschitz and J. G. Korner, Phys. Rev. D **14**, 3063 (1976).
- [56] E. P. Biernat, F. Gross, M. T. Peña and A. Stadler, Phys. Rev. D **89**, 016005 (2014) [arXiv:1310.7545 [hep-ph]].
- [57] R. A. Gilman and F. Gross, J. Phys. G **28**, R37 (2002) [nucl-th/0111015].
- [58] J. J. Kelly, Phys. Rev. C **56**, 2672 (1997).
- [59] Z. Batiz and F. Gross, Phys. Rev. C **58**, 2963 (1998) [arXiv:nucl-th/9803053].
- [60] F. Gross, G. Ramalho and M. T. Peña, Phys. Rev. C **77**, 035203 (2008).
- [61] N. Isgur, G. Karl Phys. Lett. B **72**, 109 (1977).
- [62] A. J. G. Hey, P. J. Litchfield, R. J. Cashmore and , Nucl. Phys. B **95**, 516 (1975).
- [63] N. Kaiser, Phys. Rev. C **68**, 025202 (2003) [nucl-th/0302072].
- [64] I. C. Cloet, D. B. Leinweber, A. W. Thomas, Phys. Lett. B **563**, 157 (2003) [hep-lat/0302008].
- [65] D. Arndt, B. C. Tiburzi and , Phys. Rev. D **69**, 014501 (2004) [hep-lat/0309013].
- [66] F. Dohrmann *et al.*, Eur. Phys. J. A **45**, 401 (2010) [arXiv:0909.5373 [nucl-ex]].
- [67] C. E. Carlson, Phys. Rev. D **34**, 2704 (1986); C. E. Carlson and J. L. Poor, Phys. Rev. D **38**, 2758 (1988).
- [68] C. E. Carlson and N. C. Mukhopadhyay, Phys. Rev. Lett. **81**, 2646 (1998) [hep-ph/9804356].
- [69] J. Beringer *et al.* [Particle Data Group Collaboration], Phys. Rev. D **86**, 010001 (2012).
- [70] I. Aznauryan, V. Braun, V. Burkert, S. Capstick, R. Edwards, I. C. Cloet, M. Giannini and T. S. H. Lee *et al.*, arXiv:0907.1901 [nucl-th].
- [71] G. Ramalho and M. T. Peña, work in preparation.